Available online at www.sciencedirect.com
SCIENCE DIRECT®
Biochemical and Biophysical Research Communications 333 (2005) 1370–1377
BBRC
www.elsevier.com/locate/ybbrc

A fast, simple method for screening radiation susceptibility genes by RNA interference ☆

Atsushi B. Tsuji [a], Hitomi Sudo [a], Aya Sugyo [a], Marika Otsuki [a], Makoto Miyagishi [b,d], Kazunari Taira [c,d], Takashi Imai [a], Yoshi-nobu Harada [a,*]

[a] *RadGenomics Project, Frontier Research Center, National Institute of Radiological Sciences, Chiba, Japan*
[b] *21st Century Center of Excellence Program, Graduate School of Medicine, The University of Tokyo, Hongo, Tokyo, Japan*
[c] *Department of Chemistry and Biotechnology, School of Engineering, The University of Tokyo, Hongo, Tokyo, Japan*
[d] *Gene Function Research Center, National Institute of Advanced Industrial Science and Technology (AIST), Central 4, 1-1-1 Higashi, Tsukuba Science City, Japan*

Received 7 June 2005
Available online 20 June 2005

Abstract

Radiotherapy can cause unacceptable levels of damage to normal tissues in some cancer patients. To understand the molecular mechanisms underlying radiation-induced physiological responses, and to be able to predict the radiation susceptibility of normal tissues in individual patients, it is important to identify a comprehensive set of genes responsible for radiation susceptibility. We have developed a simple and rapid 96-well screening protocol using cell proliferation assays and RNA interference to identify genes associated with radiation susceptibility. We evaluated the performance of alamarBlue-, BrdU-, and sulforhodamine B-based cell proliferation assays using the 96-well format. Each proliferation assay detected the known radiation susceptibility gene, *PRKDC*. In a trial screen using 28 shRNA vectors, another known gene, *CDKN1A*, and one new radiation susceptibility gene, *ATP5G3*, were identified. Our results indicate that this method may be useful for large-scale screens designed to identify novel radiation susceptibility genes.

Keywords: X-rays; Ionizing radiation; Radiotherapy; Cell cycle; DNA repair; RNA interference

Radiotherapy is used widely and successfully to treat many malignant tumor types. However, in some patients radiotherapy causes unacceptable levels of damage to normal tissues, including marked atrophy, severe edema, severe fibrosis, and dysfunction [1–3]. Variations in X-ray susceptibility may be attributed to a variety of genetic and environmental factors, including age, lifestyle, nutritional status, medication, and morbidity due to other diseases. For example, the genes responsible for ataxia telangiectasia and Nijmegen breakage syndrome are also involved in radiation susceptibility [1,2]. However, the genetic factors responsible for susceptibility in non-syndromic patients remain elusive. Although several genes related to DNA repair, cell cycle regulation, cell growth, cell death, carcinogenesis, and tumor suppression are suspected to have a role in radiation susceptibility [1–6], at present there is no clear evidence for a relationship between such genes and radiation susceptibility in cancer patients. Consequently, a comprehensive survey of genes involved in radiation susceptibility would help elucidate the molecular

☆ *Abbreviations:* *PRKDC*, protein kinase, DNA-activated, catalytic polypeptide; *CDKN1A*, cyclin-dependent kinase inhibitor 1A; *ATP5G3*, ATP synthase, H^+ transporting, mitochondrial F0 complex, subunit c (subunit 9) isoform 3; *CDC20*, CDC20 cell division cycle 20 homolog (*S. cerevisiae*); *CHC1*, regulator of chromosome condensation 1.

* Corresponding author. Fax: +81 43 206 4138.
E-mail address: y_harada@nirs.go.jp (Y. Harada).

0006-291X/$ - see front matter © 2005 Elsevier Inc. All rights reserved.
doi:10.1016/j.bbrc.2005.06.047

mechanisms underlying the physiological responses to radiation. An understanding of radiation-induced responses will enable development of genetic-based assays that could be used to predict the radiation susceptibility of normal tissues in individual patients. Knowledge gained from such assays may contribute to personalized curative radiotherapy protocols for cancer patients based on individual radiation susceptibilities [1–3].

With the completion of the human genome project, we now face the task of elucidating the functions of the identified genes. For this purpose, several genomic approaches have used RNA interference (RNAi) [7], particularly for genome-wide screening in mammals. For example, Paddison et al. [8] and Berns et al. [9] have established powerful tools for RNAi-based large-scale functional screening in mammalian cells. Also, Miyagishi et al. [10,11] have constructed a short hairpin RNA (shRNA) library against the human transcriptome. In the near future, the availability of such shRNA libraries for whole human transcripts will facilitate functional screening of any biological process [8–12].

The colony-forming assay is traditionally used to measure cellular radiation susceptibility and is the accepted standard cell survival assay in radiation biology. However, the colony-forming assay requires long-term culture (usually 10–21 days) and is difficult to automate for large-scale screening purposes (e.g., whole-genome functional screens) [13]. Moreover, the assay is limited by the fact that it is based on colony formation and is therefore less reliable for cells having low colony-forming capacity. These disadvantages illustrate the need to develop alternative radiation susceptibility assays for large-scale screening purposes. Several researchers have reported the use of cell proliferation assays, such as tetrazolium (MTT)- and sulforhodamine B (SRB)-based assays [13–18], as an alternative to the colony forming assay for measurement of radiation susceptibility in cultured cells. These cell proliferation assays are amenable to automation and have the potential to facilitate high-throughput screening of whole human transcripts. A previous report [16] indicated that the SRB assay offers practical and biological advantages over the MTT assay. In the present study, we used three cell proliferation assays, including SRB, with shRNA vectors to develop a rapid and simple 96-well protocol for screening radiation susceptibility genes.

Materials and methods

Cell culture and transfection conditions. HeLa cells (RCB0007, RIKEN BioResource Center, Tsukuba, Japan) were maintained in α-modified MEM (Sigma, St. Louis, MO) supplemented with 10% fetal calf serum (JRH Biosciences, Lenexa, KS), 2 mM L-glutamine (Invitrogen, Carlsbad, CA), 50 U/ml penicillin, and 50 μg/ml streptomycin. Cells (1×10^5) were seeded in 3.5-cm dishes. After 24 h, cells were transfected with 1 μg shRNA vectors using the TransIT-HeLaMONSTER transfection kit (Mirus, Madison, WI) according to the manufacturer's instructions. To obtain stable transfectants, cells were maintained in culture medium containing 1.5 μg/ml puromycin for two weeks.

For the 96-well screening assay, 5000 HeLa cells were seeded in each well. After 24 h, cells were transfected with 100 ng shRNA vectors using the TransIT-HeLaMONSTER transfection kit.

shRNA vectors. The pcPURhU6icas vector is a hairpin-type siRNA vector carrying the human U6 promoter and a selectable puromycin resistance marker [10,11,19]. To develop a simple and rapid radiation susceptibility assay, we constructed an shRNA vector directed against human *PRKDC* using a previously described *PRKDC* target sequence [20]. For the initial screening for radiation susceptibility genes, we selected target sites for 28 genes (see Supplementary Table 1) using an algorithm, as described [10]. Oligonucleotides were synthesized, annealed, and ligated as described previously [10,11,19].

Quantitative real-time RT-PCR. Total RNA was isolated from mock-, pcPURhU6icas-, and shRNA-transfected cells using the RNeasy Mini kit (Qiagen, Hilden, Germany). cDNA was synthesized from 1 μg total RNA using an oligo(dT) primer and the SuperScript First-Strand Synthesis system for RT-PCR (Invitrogen), according to the manufacturer's instructions. Real-time PCR amplifications were performed in an iCycler (Bio-Rad, Hercules, CA) using 2.5 μl cDNA (diluted 1:5), gene-specific primer sets for target genes and β-actin, and iQ SYBR Green supermix, according to the manufacturer's instructions. Gene expression was quantified by reference to a calibration curve generated using duplicate serial dilutions (ranging from 10^7 to 10^1 molecules) of the control plasmid. The primers used were as follows: *PRKDC*, 5′-GGATGTGTTTGTCAAGGAGCC and 5′-CCCA CTCTCTGGTTCTTGG; *ATP5G3*, 5′-ACGTCGCCTGTCACCCA ATA and 5′-TGGTCGAGATAACACTGATGCAGA; *CDC20*, 5′-GGCCAGTGGTGGTAATGATAACTTG and 5′-CCTGTTGCCA G GACATTGGA; *CDKN1A*, 5′-ACCTTCCTCATCCACCCCA and 5′-TGACTCCTTGTTCCGCTGC; and β-actin, 5′-GTGCTCGCGCT ACTCTCTCT and 5′-TCAATGTCGGATGGATGAAA. Expression levels were normalized to that measured for β-actin. Three independent experiments were performed for each target.

X-irradiation and cell proliferation assays. Three days post-transfection, mock- and shRNA-transfected cells were irradiated with 2 or 4 Gy using a Pantak HF320S (Shimadzu, Kyoto, Japan) before seeding for the four assays. For colony-forming assays, 200 mock- and 500 shRNA-transfected cells were seeded in 6-cm dishes in triplicate, and the cells were incubated for 10 days after irradiation. Cells were then fixed with methanol and stained with crystal violet. Then, the number of colonies containing more than 50 cells was counted independently by two researchers.

For cell proliferation assays, cells were seeded into 96-well plates at 1000 cells/well, in duplicate. Five days after irradiation, alamarBlue (alamarBlue reagent; TREK Diagnostic Systems, Cleveland, OH), BrdU (BrdU-based Cell Proliferation ELISA kit; Roche Applied Sciences, Indianapolis, IN), and SRB (sulforhodamine B-based Toxicology Assay kit; Sigma) assays were performed according to the manufacturer's instructions. For the alamarBlue assay, 10 μl alamarBlue reagent was added to each well, and the cells were incubated for 3 h. Absorbance at 570 and 600 nm was then measured using a Benchmark microplate reader (Bio-Rad). For the BrdU assay, 10 μl of 100 μM BrdU was added, to each well, and the cells were incubated for 4 h. After removal of the medium, cells were fixed and the DNA denatured using the FixDenat reagent (Roche Applied Sciences). After 30 min, the FixDenat reagent was removed, anti-BrdU-POD solution was added and the plate was incubated for 90 min at room temperature. The cells were then washed three times with wash solution, after which 100 μl of the substrate solution was added, and absorbance was measured at 370 and 490 nm using a microplate reader. For the SRB assay, 25 μl of trichloroacetic acid was added to each well, and the

plate was incubated for 1 h at 4 °C. After removal of the medium, 50 μl of 0.4% sulforhodamine B solution was added, and the cells were stained for 30 min at room temperature. Each well was then rinsed three times with 10% acetic acid, after which 100 μl of 10 mM Tris–base solution was added, and absorbance was measured at 570 and 655 nm using an Ultramark microplate reader (Bio-Rad). Three independent transfections were performed for each assay.

96-Well screening assay. HeLa cells were transfected with shRNA or pcPURhU6icas vectors (or no vector, for mock transfections) using the 96-well format protocol, as mentioned above. Three days post-transfection, ~1000 cells/well were seeded in three 96-well plates using an EDR-384S multichannel dispenser (BioTec, Tokyo, Japan). Two plates were irradiated at 2 or 4 Gy, respectively. After 5 days of additional culture, the SRB assay was performed.

Statistical analysis. For the colony-forming assay, cell survival was calculated as follows: plating efficiency of irradiated cells divided by the plating efficiency of non-irradiated cells (plating efficiency is defined as the number of colonies divided by the number of initially seeded cells). For cell proliferation assays, cell survival was calculated as the ratio of the OD obtained for irradiated cells to that for non-irradiated cells. Survival of non-irradiated cells was defined as 100%. The data correspond to means ± SEM and were analyzed by the Student's t test or by ANOVA with the Student–Newman–Keuls method multiple comparison test.

Results and discussion

PRKDC-shRNA vector

The *PRKDC* gene encodes the catalytic subunit of a nuclear DNA-dependent serine/threonine protein kinase that plays an important role in DNA repair [4]. In a previous study [20], a reduction in *PRKDC* gene expression was detected 72 h post-transfection with *PRKDC*-siRNA, and the *PRKDC*-knockdown cells were highly susceptible to radiation compared with mock-transfected cells [20]. To confirm the knockdown effect of our *PRKDC*-shRNA vector, we used quantitative real-time RT-PCR to measure *PRKDC* expression in mock and transiently *PRKDC*-shRNA-transfected HeLa cells at 24, 48, 72, and 96 h post-transfection. At these time points, expression of the *PRKDC* gene was reduced to 6.4 ± 2.0%, 0.9 ± 0.5%, 5.0 ± 2.2%, and 15.5 ± 4.6%, respectively, in *PRKDC*-shRNA-transfected cells compared with mock-transfected cells. Thus, high-level

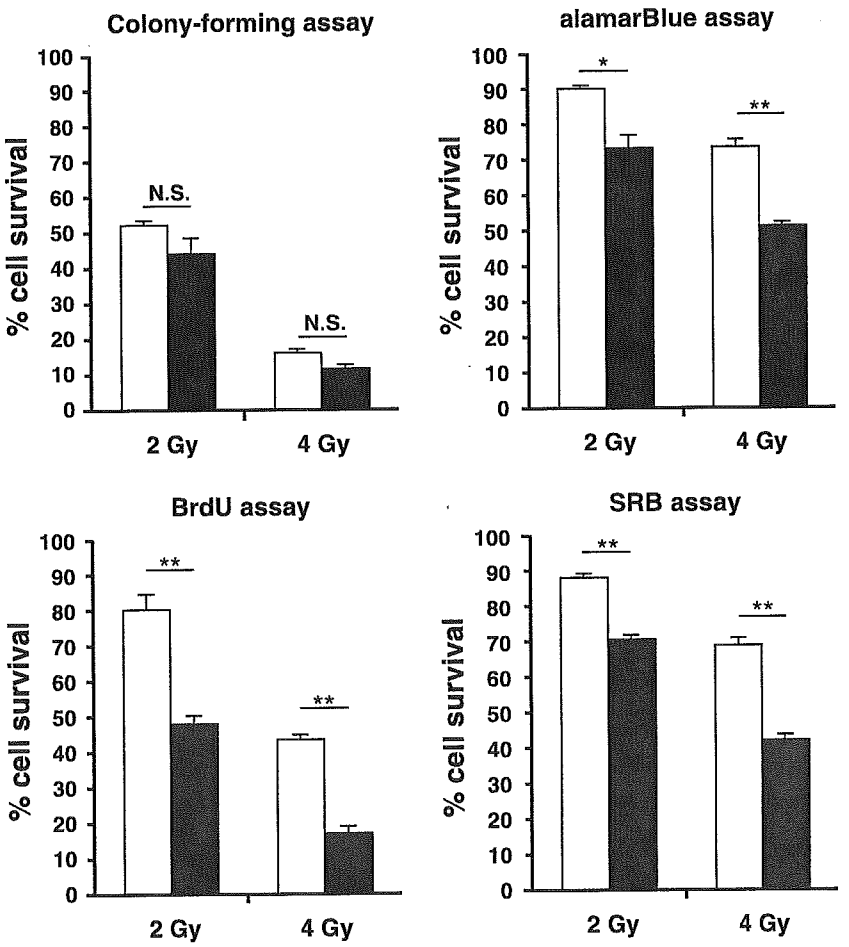

Fig. 1. Survival of mock-transfected (white bars) and *PRKDC*-shRNA-transfected (black bars) HeLa cells measured using the alamarBlue, BrdU, SRB, and colony-forming assays. HeLa cells were transfected in 3.5-cm dishes and cultured for three days. After irradiation with 2 or 4 Gy, cells were seeded in 6-cm dishes (colony-forming assay) or 96-well plates (other assays). Cells were cultured for 10 days (colony-forming assay) or five days (other assays), after which we performed the assays. Survival of non-irradiated cells was defined as 100%. Data represent means ± SEM of three experiments and were analyzed using the Student's t test (**$P < 0.01$; *$P < 0.05$; NS, not significant).

knockdown (>90% reduction) was achieved for at least 72 h after transfection. We therefore performed transient transfection experiments 72 h after transfection with the *PRKDC*-shRNA vector.

Radiation susceptibility assays

Genes that are strongly associated with radiation susceptibility are likely to affect cell survival or growth, because these are most basic of biological responses after irradiation. We chose three cell proliferation assays, based on alamarBlue, BrdU or sulforhodamine B (SRB), to develop a simple method for detecting radiation susceptibility genes. The alamarBlue assay qualitatively measures the proliferation of cultured cells based on metabolic activity. The alamarBlue reagent, an oxidation–reduction indicator, undergoes a colorimetric change in response to chemical reduction of the growth medium as a result of cell growth [21]. The BrdU assay quantitates cell proliferation based on the measurement of BrdU incorporation during DNA synthesis in proliferating cells [22]. The SRB assay determines total biomass by staining cellular proteins [13,16,17].

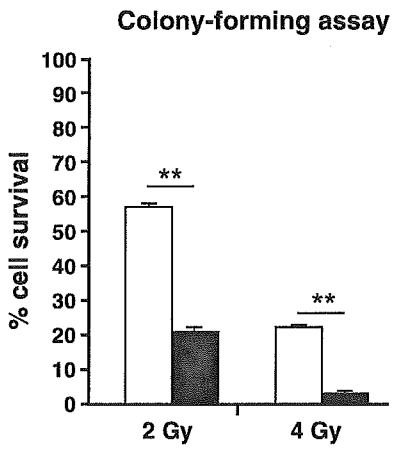

Fig. 2. Survival of stable *PRKDC*-shRNA-knockdown (black bars) and untreated (white bars) HeLa cells after radiation exposure. After irradiation with 2 or 4 Gy, cells were seeded in 6-cm dishes in triplicate. Survival was assessed 10 days post-irradiation using the colony-forming assay. Survival of non-irradiated cells was defined as 100%. The data correspond to means ± SEM of three experiments and were analyzed by the Student's *t* test (**$P < 0.01$).

In previous studies that used a 96-well assay format to determine the radiation susceptibilities of various cell lines, Griffon et al. [16] and Banasiak et al. [17] seeded ~300 cells/well and cultured the cells for 10 and 14 days after irradiation, respectively. The purpose of these studies was to develop alternative radiation susceptibility assays that were closely correlated with the colony-forming assay. Therefore, they chose >10-day incubation times (i.e., >6 cell doubling times) and very low cell densities (300 cells/well). In contrast, our primary purpose was to develop an assay for detecting radiation susceptibility genes that was suitable for large-scale screening with shRNA libraries. Thus, it was important that our assay accurately detect radiation susceptibility genes, but it was not essential that the results correlate with the colony-forming assay. Moreover, the ability of some shRNA knockdown cells to form colonies (plating efficiency) could be reduced. Given that the plating efficiency of *PRKDC*-shRNA-transfected cells was reduced by ~60% compared with mock-transfected cells (Supplementary Fig. 1), we based our assay on standard cell densities and seeded 1000 cells/well (30–40% confluence) in order to obtain greater numbers of surviving cells—and thus screen more genes—including those that strongly affect cell growth. To determine the optimal post-seeding incubation time for each cell proliferation assay, we analyzed cells at days 3, 5, and 7 after seeding in 96-well plates (1000 cells/well) without exposure to ionizing radiation (data not shown). The results showed that a 5-day incubation after seeding was optimal for all three cell proliferation assays. Fig. 1 shows survival after irradiation with 2 or 4 Gy, determined using the colony-forming assay and all three cell proliferation assays. Results from the colony-forming assay indicated that survival of *PRKDC*-shRNA-transfected cells was apparently reduced compared with mock-transfected cells, but the difference was not statistically significant. However, results from all three cell proliferation assays indicated a significant reduction in survival of *PRKDC*-shRNA-transfected cells compared with mock-transfected cells at both radiation doses. The colony-forming assay failed

Table 1
Summary of the radiation susceptibility assays used in this study

Assay	Sensitivity[a]	Procedure[b]	Time[c]	Cost	Storage[d]	Measurement	Automation[e]
alamarBlue	High	Very easy	5	Low	Impossible	Plate reader	Simple
BrdU	Very high	Laborious	5	High	Possible	Plate reader	Simple
SRB	Very high	Easy	5	Low	Possible	Plate reader	Simple
Colony-forming	Low	Very laborious	10	Low	Possible	Manual counting	Difficult

[a] Sensitivity of determining survival of *PRKDC*-knockdown cells.
[b] Very high: $P < 0.01$ at both 2 and 4 Gy; high: $P < 0.01$ at 2 or 4 Gy; low: survival was apparently reduced, but not significantly.
[c] Number of days post-irradiation that the assay was performed.
[d] The possibility of stopping and storing during the assay.
[e] Full- or semi-automated assay procedure from seeding to measurement.

to detect a statistically significant difference between survival of *PRKDC*-knockdown and mock-transfected cells in these transient knockdown experiments, but did detect a significant difference in stably transfected cells (Fig. 2). There are two possible explanations for these results. First, the colony-forming assay measures the proliferation of a single cell and could therefore be more strongly affected by untransfected cells (transfection efficiency was 60–70%) compared with the other three assays. Second, the period of the high-level knockdown effect of the *PRKDC*-shRNA vector could be too short for the colony-forming assay. Our results suggest that the three cell proliferation assays tested here have great utility for shRNA-based large-scale screening of radiation susceptibility genes.

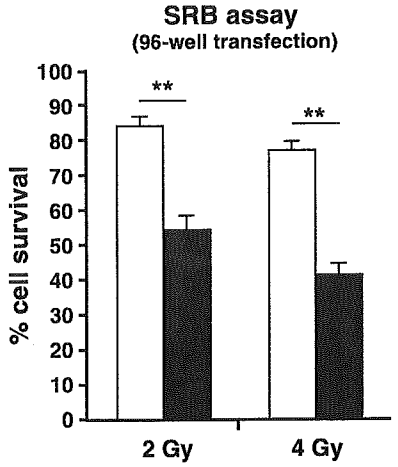

Fig. 3. Survival of mock-transfected (white bars) and *PRKDC*-shRNA-transfected (black bars) HeLa cells measured using 96-well screening protocol (the SRB assay with transfection in the 96-well plate). HeLa cells were transfected with mock (white bars) and *PRKDC*-shRNA (black bars) in the 96-well plate and were seeded into three new 96-well plates three days after transfection. Two plates were irradiated at 2 or 4 Gy, respectively. Five days post-irradiation, cell survival was measured by the 96-well SRB assay. Survival of non-irradiated cells was defined as 100%. Data represent means ± SEM of three experiments and were analyzed using the Student's *t* test (**$P < 0.01$).

The four types of radiation susceptibility assay used in this study are summarized in Table 1. The BrdU assay was the most sensitive in the transient shRNA-transfection experiment, but this assay is also laborious and expensive. The alamarBlue and SRB assays are simple, inexpensive, and sufficiently sensitive to identify radiation susceptibility genes. The alamarBlue assay is particularly simple in that it involves merely adding the alamarBlue reagent to living cells. The BrdU and SRB assays can be stopped temporarily and stored during assay procedures, an important advantage over the alamarBlue assay for large-scale screening procedures. Results from all three cell proliferation assays were achieved in half the number of days (after irradiation) required for the colony-forming assay. Moreover, the cell proliferation assays can be fully automated from seeding to measurement. Although each proliferation assay has its merits and shortcomings, our results demonstrate that all three assays were suitable for detecting radiation susceptibility genes using the shRNA vector (see Fig. 1).

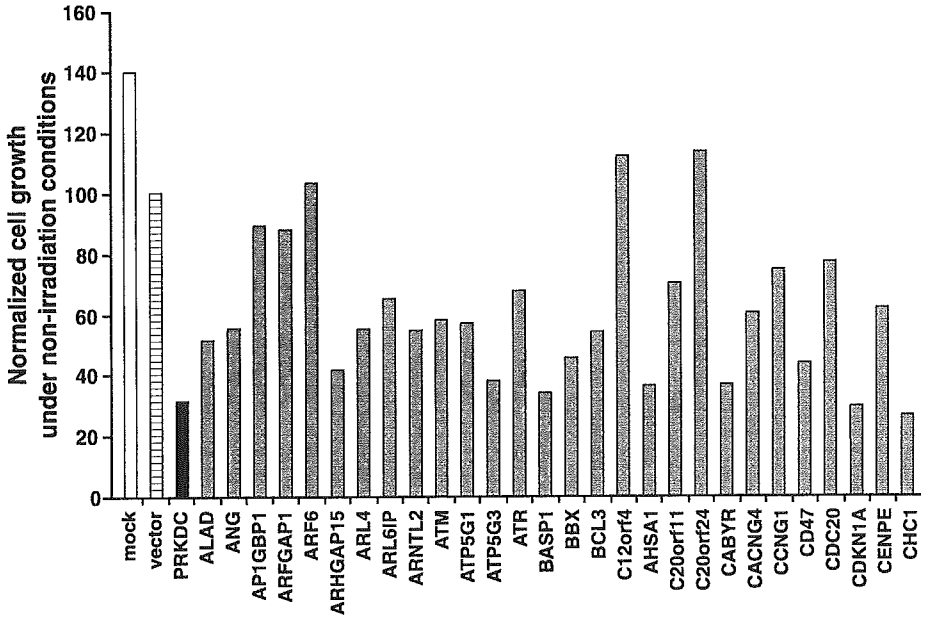

Fig. 4. Cell growth after knockdown of 28 genes under non-irradiation conditions using the 96-well screening protocol. HeLa cells were transfected with mock (white bars), pcPURhU6icas (vector, horizontal striped bars), *PRKDC*-shRNA (black bars), or shRNAs targeted against 28 genes (gray bars; gene information shown in Supplementary Table 1) in the 96-well plate and were seeded into a new 96-well plate three days after transfection. Five days after seeding, cell growth was measured by the 96-well SRB assay. Cell growth of pcPURhU6icas-transfected cells was defined as 100%.

96-Well screening assay

Transfection in a 96-well format is essential for sufficient throughput during large-scale screening. We performed a trial screen using the 96-well format SRB cell proliferation assay with the 96-well format transfection and a multichannel dispenser. Survival of *PRKDC*-shRNA-transfected cells irradiated with 2 or 4 Gy was significantly reduced compared with that of mock-transfected cells (Fig. 3). Although the coefficient of variation (CV) of transfection in the semi-automated screening protocol (5.2–25.7%) was higher than that of the manual protocol (1.2–6.2%), the screening protocol had sufficient sensitivity to detect genes that strongly affect radiation susceptibility, such as *PRKDC*. To examine whether other radiation susceptibility genes could be

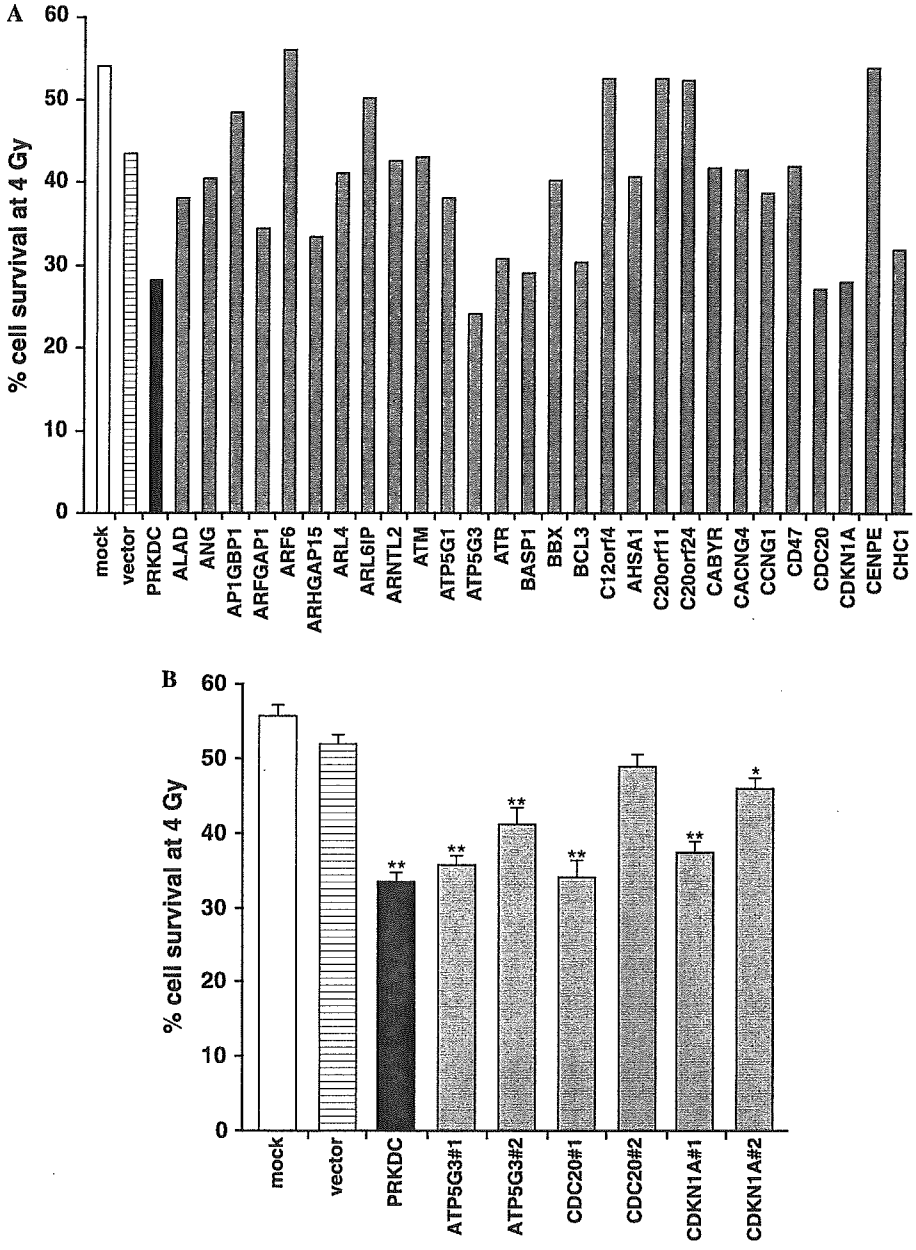

Fig. 5. (A) Screening of 28 genes using the 96-well screening protocol. Survival of HeLa cells transfected with mock (white bars), pcPURhU6icas (vector, horizontal striped bars), *PRKDC*-shRNA (black bars), or shRNAs targeted against 28 genes (gray bars; gene information shown in Supplementary Table 1) was measured five days after radiation exposure at 4 Gy. Cell survival of non-irradiated cells was defined as 100%. The survival of *PRKDC*-shRNA-transfected cells was 28.2%. (B) Survival of mock-transfected HeLa cells (white bars) and HeLa cells transfected with pcPURhU6icas (vector, horizontal striped bars), *PRKDC*-shRNA (black bars), *ATP5G3* (gray bars), *CDC20* (gray bars), or *CDKN1A* (gray bars) shRNAs. Survival was measured using the SRB assay with transfection in 3.5-cm dishes. Survival of non-irradiated cells was defined as 100%. Data correspond to means ± SEM of three experiments and were analyzed by ANOVA with the Student–Newman–Keuls method multiple comparison test (vs. vector, $^{**}P < 0.01$ and $^{*}P < 0.05$).

detected using the screening protocol, we performed a small-scale screen with part of our RNAi library, including 28 shRNA vectors against 28 genes (Supplementary Table 1). To examine the effects of knockdown on growth, we measured the growth of cells transfected with mock, pcPURhU6icas (no insert), or these 28 shRNA vectors under non-irradiation conditions using the SRB screening protocol (Fig. 4). The growth of cells transfected with pcPURhU6icas was reduced by ~40% compared with mock-transfected cells, suggesting that the vector DNA is somewhat cytotoxic. The growth of *PRKDC*-shRNA-transfected cells was markedly reduced by ~70% compared with that of pcPURhU6icas-transfected cells, consistent with the plating efficiency data (~60% reduction, as mentioned above). The growth of cells transfected with 28 shRNA vectors was between 27% and 114% compared with that of pcPURhU6icas-transfected cells, suggesting that the genes affect growth to varying degrees. The growth of cells transfected with 26 of the 28 shRNA vectors was greater than that of *PRKDC*-shRNA-transfected cells. The growth of cells transfected with the two other shRNA vectors, however, was less than that of *PRKDC*-shRNA-transfected cells (which was 32% compared with that of pcPURhU6icas-transfected cells). These two shRNAs were targeted against the genes *CDKN1A* (29% relative growth) and *CHC1* (27%). Because these differences in growth appeared to be minor compared with that of *PRKDC*-shRNA-transfected cells, we performed the radiation susceptibility screening assay in these cells after irradiation at 4 Gy. Cell survival of mock-, pcPURhU6icas-, and *PRKDC*-shRNA-transfected cells was 54.0%, 43.5%, and 28.2%, respectively, and that of cells transfected with the 28 shRNA vectors ranged between 24% and 56% (Fig. 5A). Survival of cells transfected with shRNA vectors targeted against the *CDKN1A*, *ATP5G3*, and *CDC20* genes was lower than that of the *PRKDC* gene (28.2%) following irradiation. The *CDKN1A* gene encodes a protein that plays a role in cell cycle regulation [23], but it is not known whether knockdown of this gene results in high susceptibility to radiation. The *ATP5G3* gene encodes a subunit of mitochondrial ATP synthase [24]. The *CDC20* gene product is associated with cell cycle regulation via the activation of an anaphase-promoting complex in G_1 phase [25]. The *ATP5G3* and *CDC20* genes have not previously been reported to be associated with radiation susceptibility.

To confirm that these three genes are associated with radiation susceptibility, we performed the SRB assay using additional shRNA vectors (Supplementary Table 1) targeted against each gene via transfection in 3.5-cm dishes. Cell survival following irradiation at 4 Gy was significantly reduced compared with both mock- and pcPURhU6icas-transfected cells for all the transfectants except *CDC20*#2 (Fig. 5B). Expression levels of each of the targeted genes in shRNA-transfected cells were reduced to 17–39% of that seen in pcPURhU6icas-transfected cells, with the exception of cells transfected with the *CDC20*#2 vector, which did not show reduced expression of *CDC20* (Supplementary Fig. 2). The insufficient gene knockdown obtained with the *CDC20*#2 vector explains why post-irradiation survival of *CDC20*#2-transfected cells was not affected. Thus, further experimentation is required to determine definitively whether *CDC20* is associated with radiation susceptibility.

Our experimental approach identified at least one new radiation susceptibility gene, *ATP5G3*, in addition to one known gene, *CDKN1A*, suggesting that the 96-well screening protocol has potential for use in large-scale screens to determine novel genes associated with radiation susceptibility using shRNA libraries. The screening procedure may potentially save costs and screening time compared with conventional methods. The screening protocol required 10% of the amount of shRNA vectors and transfection reagents needed for assays in larger plates; moreover, it required half the post-irradiation incubation time compared with the traditional colony-forming assay. Therefore, this simple and rapid method may be highly effective for large-scale screening of novel radiation susceptibility genes. Toward this end, we plan to construct an shRNA library against whole human transcripts [10,11] and utilize it in our screening protocol. The large-scale identification of novel radiation susceptibility genes may help elucidate the molecular mechanisms underlying the physiological responses to X-ray exposure. Moreover, the identification of genes associated with radiation susceptibility may potentially lead to the development of genetic-based assays that can be used to predict the radiation susceptibility of normal tissues in individual patients.

Acknowledgments

This research was supported in part by grants from the Ministry of Education, Culture, Sports, Science and Technology of Japan (Nos. 14580805 and 16500282).

Appendix A. Supplementary data

Supplementary data associated with this article can be found, in the online version, at doi:10.1016/j.bbrc.2005.06.047.

References

[1] N.S. Russell, A.C. Begg, Editorial radiotherapy and oncology 2002: predictive assays for normal tissue damage, Radiother. Oncol. 64 (2002) 125–129.

[2] C.N. Andreassen, J. Alsner, J. Overgaard, Does variability in normal tissue reactions after radiotherapy have a genetic basis—where and how to look for it?, Radiother. Oncol. 64 (2002) 131–140.
[3] M. Iwakawa, T. Imai, Y. Harada, S. Ban, Y. Michikawa, K. Saegusa, M. Sagara, A. Tsuji, S. Noda, A. Ishikawa, RadGenomics project, Nippon Igaku Hoshasen Gakkai Zasshi 62 (2002) 484–489.
[4] J.H. Hoeijmakers, Genome maintenance mechanisms for preventing cancer, Nature 411 (2001) 366–374.
[5] G. Iliakis, Y. Wang, J. Guan, H. Wang, DNA damage checkpoint control in cells exposed to ionizing radiation, Oncogene 22 (2003) 5834–5847.
[6] B.G. Haffty, P.M. Glazer, Molecular markers in clinical radiation oncology, Oncogene 22 (2003) 5915–5925.
[7] S.M. Elbashir, J. Harborth, W. Lendeckel, A. Yalcin, K. Weber, T. Tuschl, Duplexes of 21-nucleotide RNAs mediate RNA interference in cultured mammalian cells, Nature 411 (2001) 494–498.
[8] P.J. Paddison, J.M. Silva, D.S. Conklin, M. Schlabach, M. Li, S. Aruleba, V. Balija, A. O'Shaughnessy, L. Gnoj, K. Scobie, K. Chang, T. Westbrook, M. Cleary, R. Sachidanandam, W.R. McCombie, S.J. Elledge, G.J. Hannon, A resource for large-scale RNA-interference-based screens in mammals, Nature 428 (2004) 427–431.
[9] K. Berns, E.M. Hijmans, J. Mullenders, T.R. Brummelkamp, A. Velds, M. Heimerikx, R.M. Kerkhoven, M. Madiredjo, W. Nijkamp, B. Weigelt, R. Agami, W. Ge, G. Cavet, P.S. Linsley, R.L. Beijersbergen, R. Bernards, A large-scale RNAi screen in human cells identifies new components of the p53 pathway, Nature 428 (2004) 431–437.
[10] M. Miyagishi, K. Taira, Strategies for generation of an siRNA expression library directed against the human genome, Oligonucleotides 13 (2003) 325–333.
[11] M. Miyagishi, S. Matsumoto, K. Taira, Generation of an shRNAi expression library against the whole human transcripts, Virus Res. 102 (2004) 117–124.
[12] A.E. Carpenter, D.M. Sabatini, Systematic genome-wide screens of gene function, Nat. Rev. Genet. 5 (2004) 11–22.
[13] B. Pauwels, A.E. Korst, C.M. de Pooter, G.G. Pattyn, H.A. Lambrechts, M.F. Baay, F. Lardon, J.B. Vermorken, Comparison of the sulforhodamine B assay and the clonogenic assay for in vitro chemoradiation studies, Cancer Chemother. Pharmacol. 51 (2003) 221–226.
[14] J. Carmichael, W.G. DeGraff, A.F. Gazdar, J.D. Minna, J.B. Mitchell, Evaluation of a tetrazolium-based semiautomated colorimetric assay: assessment of radiosensitivity, Cancer Res. 47 (1987) 943–946.
[15] P. Price, T.J. McMillan, Use of the tetrazolium assay in measuring the response of human tumor cells to ionizing radiation, Cancer Res. 50 (1990) 1392–1396.
[16] G. Griffon, J.L. Merlin, C. Marchal, Comparison of sulforhodamine B, tetrazolium and clonogenic assays for in vitro radiosensitivity testing in human ovarian cell lines, Anticancer Drugs 6 (1995) 115–123.
[17] D. Banasiak, A.R. Barnetson, R.A. Odell, H. Mameghan, P.J. Russell, Comparison between the clonogenic, MTT, and SRB assays for determining radiosensitivity in a panel of human bladder cancer cell lines and a ureteral cell line, Radiat. Oncol. Investig. 7 (1999) 77–85.
[18] A.R. Barnetson, D. Banasiak, R.J. Fisher, H. Mameghan, J.C. Ribeiro, K. Brown, J.L. Brown, S.M. O'Mara, P.J. Russell, Heterogeneity of in vitro radiosensitivity in human bladder cancer cells, Radiat. Oncol. Investig. 7 (1999) 66–76.
[19] M. Miyagishi, K. Taira, U6 promoter-driven siRNAs with four uridine 3′ overhangs efficiently suppress targeted gene expression in mammalian cells, Nat. Biotechnol. 20 (2002) 497–500.
[20] Y. Peng, Q. Zhang, H. Nagasawa, R. Okayasu, H.L. Liber, J.S. Bedford, Silencing expression of the catalytic subunit of DNA-dependent protein kinase by small interfering RNA sensitizes human cells for radiation-induced chromosome damage, cell killing, and mutation, Cancer Res. 62 (2002) 6400–6404.
[21] S.L. Voytik-Harbin, A.O. Brightman, B. Waisner, C.H. Lamar, S.F. Badylak, Application and evaluation of the alamarBlue assay for cell growth and survival of fibroblasts, In Vitro Cell. Dev. Biol. Anim. 34 (1998) 239–246.
[22] T. Porstmann, T. Ternynck, S. Avrameas, Quantitation of 5-bromo-2-deoxyuridine incorporation into DNA: an enzyme immunoassay for the assessment of the lymphoid cell proliferative response, J. Immunol. Methods 82 (1985) 169–179.
[23] F. Bunz, A. Dutriaux, C. Lengauer, T. Waldman, S. Zhou, J.P. Brown, J.M. Sedivy, K.W. Kinzler, B. Vogelstein, Requirement for p53 and p21 to sustain G2 arrest after DNA damage, Science 282 (1998) 1497–1501.
[24] W.L. Yan, T.J. Lerner, J.L. Haines, J.F. Gusella, Sequence analysis and mapping of a novel human mitochondrial ATP synthase subunit 9 cDNA (ATP5G3), Genomics 24 (1994) 375–377.
[25] G. Fang, H. Yu, M.W. Kirschner, Direct binding of CDC20 protein family members activates the anaphase-promoting complex in mitosis and G1, Mol. Cell 2 (1998) 163–171.

Oncogene (2005) 24, 662–671

www.nature.com/onc

Smad4 silencing in pancreatic cancer cell lines using stable RNA interference and gene expression profiles induced by transforming growth factor-β

Amarsanaa Jazag[1], Hideaki Ijichi[1], Fumihiko Kanai*[,1,2], Takaaki Imamura[1,3], Bayasi Guleng[1], Miki Ohta[1], Jun Imamura[1], Yasuo Tanaka[1], Keisuke Tateishi[1], Tsuneo Ikenoue[1,4], Takayuki Kawakami[1], Yoshihiro Arakawa[2], Makoto Miyagishi[5,6], Kazunari Taira[5,6], Takao Kawabe[1] and Masao Omata[1]

[1]*Department of Gastroenterology, Graduate School of Medicine, University of Tokyo, 7-3-1, Hongo, Bunkyo-ku, Tokyo 113-8655, Japan;* [2]*Clinical Research Center, University of Tokyo Hospital, Tokyo 113-8655, Japan;* [3]*Department of Medicine and Clinical Oncology, Graduate School of Medicine, Chiba University, Chiba 260-0870, Japan;* [4]*Division of Gastroenterology, Institute for Adult Diseases, Asahi Life Foundation, Tokyo 160-0023, Japan;* [5]*Department of Chemistry and Biotechnology, Graduate School of Engineering, University of Tokyo, Tokyo 113-8656, Japan;* [6]*Gene Function Research Center, National Institute of Advanced Industrial Science and Technology, Ibaraki 305-8562, Japan*

The transforming growth factor-β (TGF-β)-Smad signaling pathway inhibits the growth of human epithelial cells and plays a role in tumor suppression. The *Smad4* gene is mutated or deleted in 50% of pancreatic cancers. In this study, we succeeded in establishing Smad4 knockdown (S4KD) pancreatic cancer cell lines using the stable RNA interference (RNAi) method. Smad4 protein expression was reduced dramatically and TGF-β-Smad signaling was markedly inhibited in the S4KD cell lines. The S4KD and control cells were stimulated with TGF-β and analysed using a cDNA microarray that contained 3756 genes, in order to screen for target molecules downstream of TGF-β. The microarray analysis revealed that 187 S4KD genes and 155 genes in the control cells were regulated immediately upon TGF-β stimulation. Quantitative RT–PCR analysis on several of these genes produced results that corroborated the outcome of the microarray analysis. Most of the genes in the S4KD and control cells identified by the array differed, which suggests signaling pathways that differ according to Smad4 status. Of the identified genes, 246 have not been reported previously as genes that lie downstream of TGF-β. Genes that are involved in cell proliferation, adhesion, and motility were found to be regulated differentially with respect to S4KD and control cells. Cell migration induced by TGF-β was inhibited in the S4KD cells, which might be associated with a different regulation of integrin β7. The knock down of a specific gene using stable RNAi appears to be a promising tool for analysing endogenous gene function.
Oncogene (2005) **24**, 662–671. doi:10.1038/sj.onc.1208102
Published online 13 December 2004

Keywords: Smad4; TGF-β; stable RNAi; cDNA microarray; pancreatic cancer

*Correspondence: F Kanai; E-mail: kanaif-int@h.u-tokyo.ac.jp
Received 16 January 2004; revised 3 August 2004; accepted 14 August 2004; published online 13 December 2004

Introduction

Smad4 is a key mediator of transforming growth factor-β (TGF-β)-Smad signaling, which is known to inhibit epithelial cell growth. Formation of a heteromeric complex between the TGF-β ligand and the TGF-β type I and type II receptors (TβRI and TβRII) leads to phosphorylation of the cytoplasmic Smad2 and Smad3 proteins by the activated TβRI kinase, which, in turn, allows the formation of a heteromeric complex with Smad4. Smad4 is the only mammalian form of the common mediator Smad (Co-Smad); the cytoplasmic Smad oligomer is translocated into the nucleus, where it regulates TGF-β-responsive gene transcription in co-operation with transcription factors and other cofactors (reviewed in Miyazono *et al.*, 2000; Derynck *et al.*, 2001).

Impairment of the Smad pathway results in escape from growth inhibition and leads to the promotion of cell proliferation, thereby contributing to carcinogenesis. Various genetic and epigenetic alterations of the components of the Smad pathway have been identified in several human cancers (Markowitz *et al.*, 1995; Hahn *et al.*, 1996; Schutte *et al.*, 1996; Togo *et al.*, 1996; Miyaki *et al.*, 1999; Wang *et al.*, 2000). Mutation or deletion of the *Smad4* gene, which was originally designated as the tumor suppressor gene *DPC4* (*deleted in pancreatic carcinoma, locus 4*), has been detected in 50% of all pancreatic cancers (Hahn *et al.*, 1996), and we have reported previously that many pancreatic cancer cell lines have impaired TGF-β-Smad signaling, due to a functionally inactivated Smad4 (Ijichi *et al.*, 2001).

The TGF-β signal is also transduced through the Smad-independent pathway (Bhowmick *et al.*, 2001; Yu *et al.*, 2002), and appears to promote tumor progression under certain conditions (Derynck *et al.*, 2001). However, the characteristics and significance

of the Smad-independent signaling pathway remain unresolved. Since increased expression of TGF-β is often detected in tumors, including pancreatic cancers (Derynck *et al.*, 1983; Friess *et al.*, 1993), it is possible that these tumors develop in a cell-autonomous manner via the TGF-β-induced, Smad4-independent pathway.

RNA interference (RNAi) is an evolutionarily conserved mechanism of gene silencing. Recently, 21- to 23-nucleotide double-stranded RNA (short interfering RNA, siRNA) molecules have been shown to exhibit specific RNAi effects without inducing the host defense system (Elbashir *et al.*, 2001). Although the effect of siRNA that is introduced transiently into cells is restricted because of low transfection efficiency or the short-term persistence of silencing effects, we, and others, have reported recently that a plasmid vector that expresses siRNA enables long-term persistence of the silencing effect, a phenomenon that is termed 'stable RNAi' (Brummelkamp *et al.*, 2002; Miyagishi and Taira, 2002). This system represents a powerful tool for analysing endogenous gene silencing.

In this study, we established Smad4 knockdown (S4KD) pancreatic cancer cell lines using the stable RNAi, subsequently investigated the Smad4-independent target genes downstream of TGF-β and phenotypic changes due to the S4KD.

Results and discussion

Establishment of S4KD pancreatic cancer cell lines

In order to mimic the genetic characteristics of inactivated Smad4 in clinical pancreatic cancer, we knocked down the *Smad4* gene in the human pancreatic cancer cell line PANC-1, which has a functional TGF-β-Smad signaling pathway (Grau *et al.*, 1997; Ijichi *et al.*, 2001). First, we constructed plasmids that expressed short hairpin RNAs that were targeted against Smad4 under the control of the U6 promoter (pcPUR + U6-Smad4i) (Figure 1) as described previously (Miyagishi and Taira, 2002; Yokota *et al.*, 2003). Five different sequences were originally selected for targeting the *Smad4* gene (Supplementary Table 1).

Second, we transiently transfected PANC-1 cells with pcPUR + U6-Smad4i and the Smad4 protein expression vector, and examined Smad4 protein expression by Western blotting. As shown in Figure 2a, the site 5 plasmid (lanes 3 and 4) was the most effective at blocking Smad4 protein expression, and was employed in subsequent experiments.

Then, PANC-1 cells were transfected with pcPUR + U6-Smad4i (site 5) or pcPUR + U6icassette (control vector), and incubated with 2 μg/ml puromycin (WAKO, Osaka, Japan), to select puromycin-resistant single clones and cell pools, which were mixtures of the puromycin-resistant polyclonal cells. Thus, we obtained S4KD and Smad4 intact (control) cell lines, which are designated as PANC-1-S4KD and PANC-1-puro, respectively. For the sake of convenience, the PANC-1-puro cells are termed the WT cells.

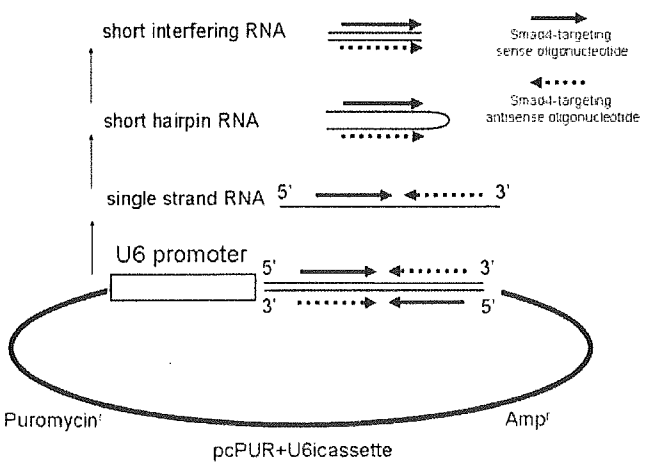

Figure 1 Design of plasmids expressing siRNA molecules targeted against Smad4. The short-hairpin RNA targeting the *Smad4* gene was expressed under the control of the U6 promoter, and was digested to form siRNA, which inhibited endogenous Smad4 expression. The transfected cells were selected with puromycin

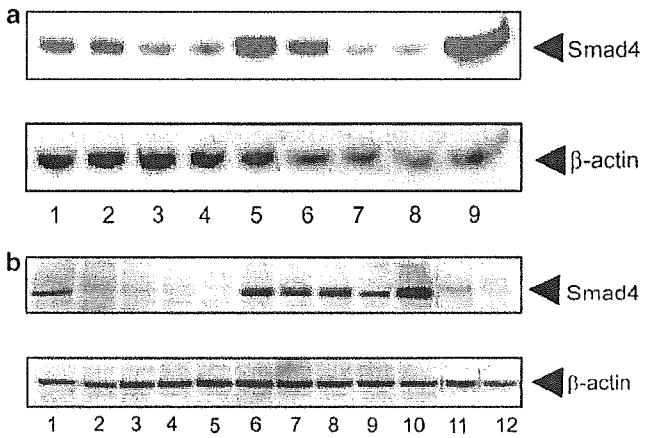

Figure 2 Western blotting showed marked reduction of Smad4 protein expression in the S4KD cells. (**a**) Screening of the most effective targeting site for the *Smad4* gene. PANC-1 cells were transiently cotransfected with the Smad4 protein expression vector (Smad4PEV) and pcPUR + U6-Smad4i in duplicate. After 48 h, equivalent amounts of protein from the total cell lysates were electrophoresed, and the Smad4 protein was detected by Western blotting. Site 5 was the most effective construct. Lanes 1 and 2, Smad4PEV and pcPUR + U6-Smad4i (site 1); lanes 3 and 4, Smad4PEV and pcPUR + U6-Smad4i (site 5); lanes 5 and 6, Smad4PEV and pcPUR + U6icassette; lanes 7 and 8, no treatment; lane 9, Smad4-positive control. (**b**) Confirmation of the endogenous S4KD. PANC-1 cells were transfected with pcPUR + U6-Smad4i or pcPUR + U6icassette; and incubated with puromycin, to select stably transfected cells. The total cell lysates of single clones or cell pools were subjected to Western blotting. Lane 1, PANC-1-S4KD clone no. 2; lane 2, S4KD clone no. 1; lane 3, S4KD clone no. 3; lane 4, S4KD clone no. 4; lane 5, S4KD clone no. 5; lane 6, WT clone no. 1; lane 7, WT clone no. 2; lane 8, WT cell pool; lane 9, PANC-1 (parental); lane 10, Smad4-positive control; lane 11, S4KD cell pool (targeted to site 1 of *Smad4*); lane 12, S4KD cell pool (site 5, used in the subsequent experiments in the present study). A representative blot is shown in (**a**) and (**b**)

As shown in Figure 2b, most of the PANC-1-S4KD clones (lanes 1–5) and cell pools (lanes 11 and 12) exhibited a dramatic knock down of Smad4 protein expression.

There are three isoforms of TGF-β, called TGF-β1, -β2, and -β3, with similar biological functions. We performed further experiments using TGF-β1 as the ligand in this study. Luciferase assays using the Smad-dependent reporter $(CAGA)_9$-luc showed that the canonical TGF-β-Smad-dependent signaling was markedly inhibited in the S4KD cells (lanes 2–6), which indicates a functional S4KD (Figure 3).

Besides, we performed several quantitative RT–PCR to confirm the status of S4KD. In the following experiments, we used the PANC-1-S4KD and WT cell pools, to avoid deriving from the specificity of a single clone. Total RNA was extracted from the S4KD and WT cell pools that were incubated with or without 10 ng/ml of TGF-β1 for 2 h. Initially, we examined the status of the Smad4 mRNA. Analysis of the S4KD and WT cells that were incubated without TGF-β revealed that Smad4 was downregulated in S4KD cells, as compared to WT cells (Figure 4a).

Recently, it has been suggested that siRNA cross-reacts with nontargeted genes that contain sequences with homology to the siRNA (Jackson *et al*., 2003). To exclude this type of phenomenon, we used quantitative RT–PCR to examine the expression of the *DCP1* (*dipeptidyl carboxypeptidase 1*) gene, which has a similar sequence to the siRNA that was targeted to the *Smad4* gene. The PANC-1-S4KD and WT cell pools showed almost identical DCP1 mRNA expression, which confirms the specificity of the S4KD in the S4KD cells (Figure 4b).

Next, we examined the expression of major Smad-dependent target molecules. Plasminogen activator inhibitor-I (PAI-I) is an extracellular matrix-associated protein, which is regulated in a Smad4-dependent manner (Hocevar *et al*., 1999). Smad7 is an inhibitory Smad, which is upregulated by TGF-β and forms a negative feedback loop (Miyazono *et al*., 2000). The WT cells showed PAI-I and Smad7 upregulation in response to TGF-β1. Conversely, induction by TGF-β1 diminished in the S4KD cells (Figure 4c and d). These results confirmed the diminished Smad4 function in the S4KD cells. The level of TGF-β1 expression did not differ between the S4KD and WT cells under basal conditions (Figure 4e). The primer sequences used for quantitative

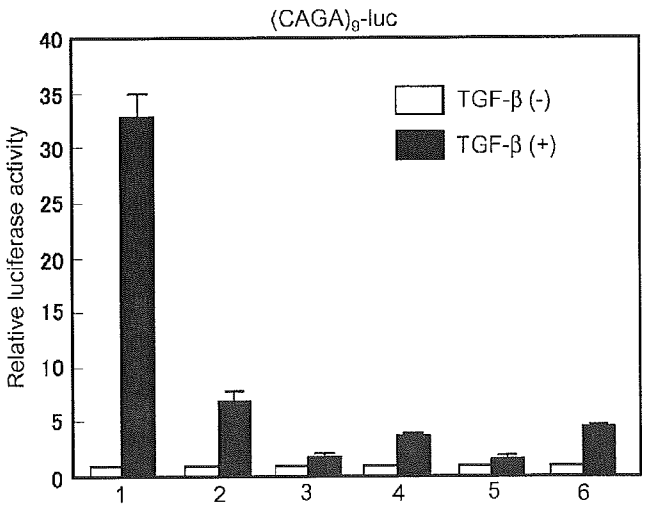

Figure 3 Inhibition of TGF-β-Smad signaling in S4KD cells. The PANC-1-S4KD and WT cells were transfected with $(CAGA)_9$-luc and pRL-SV40. After 24 h, the cells were incubated with or without 2.5 ng/ml TGF-β1 for an additional 24 h, and the dual luciferase assay was performed. The firefly luciferase activity of $(CAGA)_9$-luc was normalized to the *Renilla* luciferase activity of pRL-SV40. The level of luciferase in cells in the absence of TGF-β1 was assigned a value of 1.0, and the relative activities were calculated. The experiments were performed twice in duplicate, and the mean and standard deviation (s.d.) are shown. Lane 1, PANC-1-WT cell pool; lane 2, S4KD cell pool; lane 3, S4KD clone no. 1; lane 4, S4KD clone no. 3; lane 5, S4KD clone no. 4; lane 6, S4KD clone no. 5; Bar, s.d.

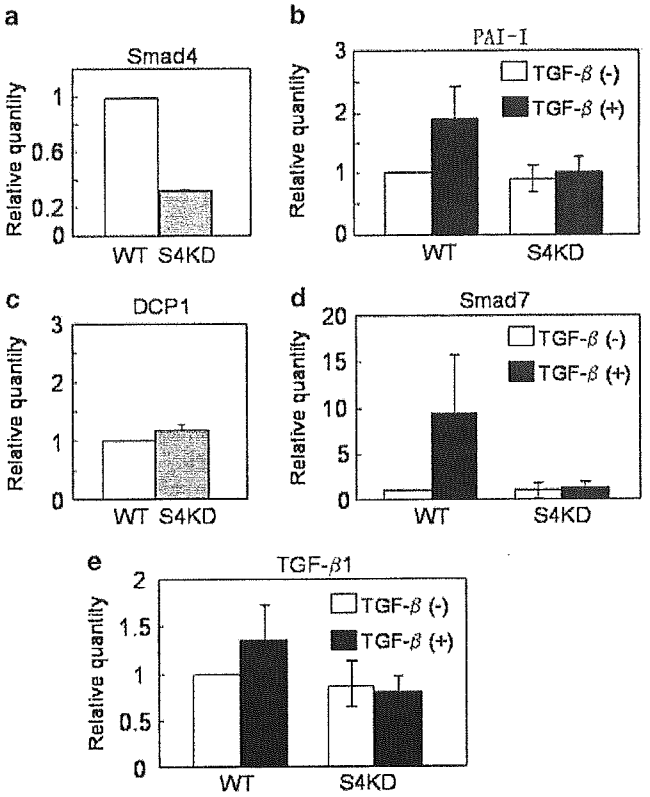

Figure 4 Quantitative RT–PCR showing Smad4-specific silencing in the S4KD cells and preserved signaling in the Smad4 intact cells. The PANC-1-S4KD and WT cell pools were incubated with or without 10 ng/ml of TGF-β1 for 2 h, and the total RNA was extracted. The cDNA templates were synthesized from 1 μg of total RNA and quantitative RT–PCR analysis was performed. The ratio of the mRNA level of each gene to that of GAPDH was calculated, and the value of 1.0 was assigned to WT cells that were incubated without TGF-β1. Each experiment was repeated twice in triplicate, and the mean and s.d. are shown. (**a**) Smad4 expression was apparently inhibited in the S4KD cells. (**b**) DCP1 expression was not inhibited in the S4KD cells. (**c**) (**d**) PAI-I and Smad7 expression was clearly induced by TGF-β1 in the WT cells, but not in the S4KD cells. (**e**) Basal TGF-β1 expression was not different between the WT and S4KD cells. Bar, s.d.

RT–PCR in this study are shown in Supplementary Table 2.

Thus, we succeeded in establishing S4KD pancreatic cancer cell lines. The stable RNAi method is considered a powerful tool for analysing the 'loss of function' of endogenous genes.

Target genes regulated by TGF-β1 in the S4KD and Smad4 intact cells

We investigated the downstream molecules that are regulated by TGF-β signaling in the S4KD cells, with the aim of developing novel target molecules or therapeutics for pancreatic cancer, which is a disease with a poor prognosis. Total RNA was also extracted from PANC-1-S4KD and WT cell pools that were incubated with or without 10 ng/ml of TGF-β1 for 2 h. We adopted the 2-h incubation in order to detect the putative direct target genes of TGF-β, the transcription of which is regulated immediately upon stimulation.

We analysed the comprehensive gene expression profiles that were induced by TGF-β1 stimulation of the S4KD and WT cells, using a microarray that contained 3756 individual genes. Comparisons of the array data in the presence and absence of TGF-β1 led to the identification of TGF-β-regulated target gene clones that showed > 2-fold increases or < 0.5-fold decreases in expression following TGF-β1 stimulation. The genes that belong to these categories are listed in Tables 1 and 2 and Supplementary Table 3.

To confirm the microarray data, we performed quantitative RT–PCR analysis on several of the genes that were obtained from the microarray. As shown in Figure 5, the RT–PCR results matched those of the array, which indicates the reliability of the detection of target genes, although less fold changes were observed in the RT–PCR than in the array in this study.

Table 1 TGF-β1- regulated genes in PANC-1-S4KD cells (partial list)

Fold change	*Gene name*	*Genbank accession no.*
18.2	Progesterone membrane binding protein	NM_006320
17.2	Nucleoporin 153 kDa	NM_005124
16.5	Snf2-related CBP activator protein	NM_006662
9.27	Kallikrein 11	NM_006853
7.60	Hypothetical protein FLJ10597	NM_016501
7.30	Dynein, axonemal, heavy polypeptide 2	U83570
6.81	Solute carrier family 23 (nucleobase transporters), member 2	NM_005847
6.70	Excision repair cross-complementing rodent repair deficiency, Complementation group 5 (xeroderma pigmentosum)	L20046
6.43	Cytochrome b-561	U06715
6.32	Variable charge, X chromosome	NM_013452
6.16	Olfactory receptor, family 10, subfamily H, member 2	NM_013939
6.15	Paired immunoglobulin-like receptor alpha	NM_013439
4.81	CDK4-binding protein p34SEI1	NM_013376
4.77	Pre-B-cell colony-enhancing factor	NM_005746
4.62	MO25 protein	NM_016289
4.58	Protein tyrosine phosphatase, receptor type, C	Y00638
4.49	Heme-binding protein	NM_015987
4.49	Methyl-CpG binding domain protein 1	Y10746
4.43	Death-associated protein 6	AF015956
4.37	CUG triplet repeat, RNA-binding protein 2	NM_006561
0.226	p21 (CDKN1A)-activated kinase 3	AF068864
0.226	Duffy blood group	U01839
0.220	Platelet-derived growth factor receptor, beta polypeptide	M21616
0.220	Cyclin E1	M73812
0.217	Absent in melanoma 2	AF024714
0.209	Proline oxidase homolog	AF010310
0.207	Spleen focus forming virus (SFFV) proviral integration oncogene spi1	NM_003120
0.204	Prepronociceptin	X97370
0.195	unc119 (*C.elegans*) homolog	NM_005148
0.183	Ras association (RalGDS/AF-6) domain family 1	NM_007182
0.177	Mitogen-activated protein kinase 7	U25278
0.174	PCTAIRE protein kinase 2	X66360
0.169	Integrin, alpha 6	X53586
0.168	Jagged 2	AF003521
0.156	Histamine receptor H2	D49783
0.152	VAMP (vesicle-associated membrane protein)-associated protein B and C	NM_004738
0.123	Guanylate cyclase 2F, retinal	L37378
0.0648	Chromosome 17 open reading frame 1A	NM_006382
0.0507	Tumor necrosis factor receptor superfamily, member 10a	NM_003844
0.0181	Hypothetical protein	NM_016479

The list includes those genes whose expression was upregulated > 2-fold or downregulated < 0.5-fold by TGF-β1. The 20 highest and the 20 lowest expressed genes are shown

Table 2 TGF-β1-regulated genes in PANC-1-puro cells (partial list)

Fold change	*Gene name*	*GenBank accession no.*
16.7	Heat shock transcription factor 2 binding protein	NM_007031
6.64	Elastin microfibril interface located protein	NM_007046
5.5	ATP-binding cassette, subfamily D (ALD), member 1	Z21876
5.37	Lysine-ketoglutarate reductase/saccharopine dehydrogenase	NM_005763
5.21	Sialidase 3 (membrane sialidase)	NM_006656
5.16	Protein kinase (cAMP-dependent, catalytic) inhibitor gamma	NM_007066
5.03	Oncostatin M	M27288
4.95	Epithelial protein upregulated in carcinoma, membrane associated protein 17	NM_005764
4.34	Cornichon-like	NM_005776
4.26	Maternal G10 transcript	NM_003910
4.16	Plasma glutamate carboxypeptidase	NM_006102
4.12	Chromosome 8 open reading frame 2	NM_007175
3.98	Cyclin E1	M73812
3.92	WNT1 inducible signaling pathway protein 3	NM_003880
3.72	Ras GTPase activating protein-like	NM_004841
3.71	Rap1 guanine-nucleotide-exchange factor directly activated by cAMP	NM_006105
3.48	Putative protein similar to nessy (Drosophila)	NM_005768
3.48	Corin	NM_006587
3.45	CUG triplet repeat, RNA-binding protein 2	NM_006561
3.35	Solute carrier family 12 (potassium/chloride transporters), member 7	NM_006598
0.401	Zinc finger protein homologous to Zfp161 in mouse	D89859
0.401	Small inducible cytokine subfamily A (Cys-Cys), member 27	NM_006664
0.399	Eukaryotic translation elongation factor 1 alpha 1	NM_001402
0.399	Ubiquitin specific protease 25	NM_013396
0.398	Liver-specific bHLH-Zip transcription factor	NM_015925
0.394	stomatin-like 2	NM_013442
0.377	Zinc finger protein 144 (Mel-18)	NM_007144
0.349	Phosphatidylserine-specific phospholipase A1alpha	NM_015900
0.339	Homeo box A2	AC004079
0.314	Hypothetical protein	NM_016465
0.289	Purinergic receptor P2X-like 1, orphan receptor	NM_005446
0.275	Ribonuclease/angiogenin inhibitor	M36717
0.264	Fibronectin leucine rich transmembrane protein 1	NM_013280
0.263	(clone PWHLC2-24) myosin light chain 2	NM_013292
0.252	Fibroblast growth factor 6	X63454
0.231	Putative tumor suppressor	NM_012191
0.229	CGI-133 protein	NM_016066
0.229	NGFI-A binding protein 2 (ERG1 binding protein 2)	NM_005967
0.214	Serine (or cysteine) proteinase inhibitor, clade F (alpha-2 antiplasmin, Pigment epithelium derived factor), member 2	D00174
0.191	Complement component 5	M65134

The list includes those genes whose expression was upregulated >2-fold or downregulated <0.5-fold by TGF-β1. The 20 highest and the 20 lowest expressed genes are shown

Figure 5a showed the examples of target genes from the S4KD cells. In the microarray the fold increase of *nucleoporin 153 kDa* was 17.2, *dynein, axonemal, heavy polypeptide 2* was 7.30, and *SUMO-1-activating enzyme subunit 2* was 2.28 in the S4KD cells, respectively. Some of the clones obtained from the S4KD array showed similar patterns of TGF-β1-mediated regulation in both the S4KD and WT cells, which suggests that certain Smad4-independent target genes are common to both cell types (Figure 5a).

Figure 5b showed representatives of target genes from the WT cells. In the microarray, the fold change of *caspase-3, apoptosis-related cysteine protease* was 2.32, *karyopherin alpha 6 (importin alpha 7)* was 2.03, and of *potassium large conductance calcium-activated channel, subfamily M, beta member 1* was 0.422 in the WT cells, respectively. The clones from the array of WT cells were regulated in a similar manner to that seen for the WT microarrays, but were not regulated in the S4KD cells, which indicates that Smad4-dependent targets are regulated only in Smad4 intact cell lines (Figure 5b).

Although the WT cells were expected to contain both the Smad4-dependent and -independent signaling pathways, they showed lower numbers of target genes than the S4KD cells. This suggests that there were more targets for TGF-β in Smad4 intact cells, especially in the Smad4-independent pathway.

Although the number of target genes in the WT cells may have been underestimated, we identified 320 clones of target molecules for TGF-β1 in this microarray analysis. In the S4KD cells, 120/3756 clones were upregulated and 67/3756 clones were downregulated by TGF-β1, which are considered Smad4-independent target genes for TGF-β (Figure 6, Table 1). In the WT cells, 116/3756 clones were upregulated and 39/3756 clones were downregulated; these may include

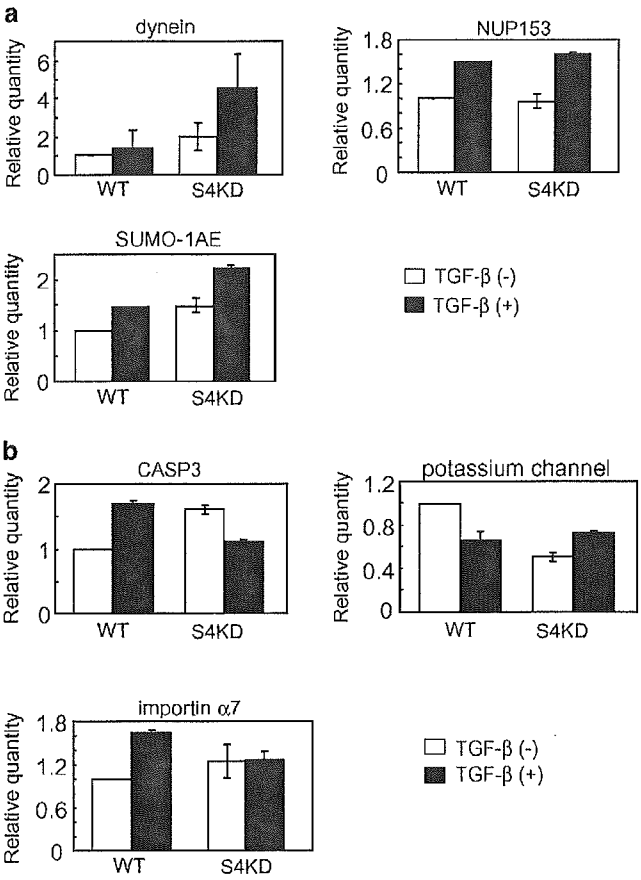

Figure 5 Quantitative RT–PCR analysis of target genes for TGF-β. The PANC-1-S4KD and WT cells were incubated with or without 10 ng/ml TGF-β1 for 2 h. Total RNA extraction, cDNA synthesis, and quantitative RT–PCR analysis were performed as described above. The ratio of the mRNA level of each gene to that of GAPDH was calculated, and the value of 1.0 was assigned to WT cells that were incubated without TGF-β1. All of the experiments were repeated twice in triplicate, and the mean and s.d. are shown. (**a**) Quantification of the genes that were obtained from the S4KD array. (**b**) Quantification of the genes that were obtained from the WT array. Dynein, dynein, axonemal, heavy polypeptide 2; SUMO-1AE, SUMO-1 activating enzyme subunit 2; NUP153, 153-kDa nucleoporin; CASP3, caspase-3; potassium channel, potassium large conductance calcium-activated channel, subfamily M, beta member 1; Bar, s.d.

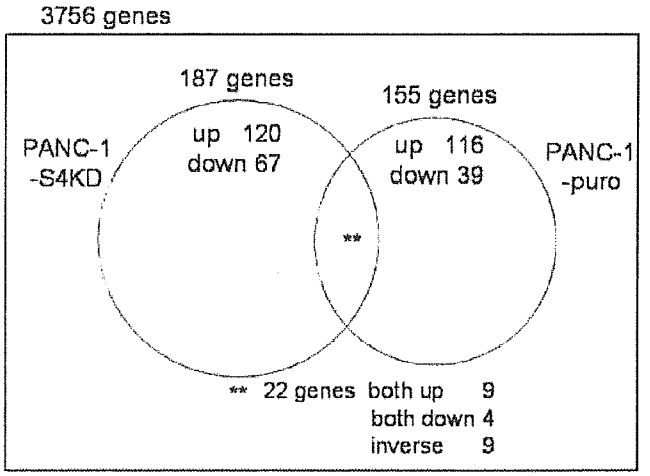

Figure 6 Targets of TGF-β signaling in the S4KD and Smad4 intact cells, as identified by microarray analysis. The PANC-1-S4KD and WT cell pools were incubated for 2 h in the presence or absence of 10 ng/ml TGF-β1, and total RNA was extracted. The fluorescent cDNA probes were prepared from each RNA sample, (i), (ii), (iii), (iv), and analysed by the microarray which consisted of 3756 distinct cDNA clones as described in Materials and methods. The analyses with probes (ii) and (i) were compared to detect clones that were putatively regulated in a Smad4-independent manner by TGF-β1. Comparison of the analyses with probes (iv) and (iii) identified clones that were putatively regulated by TGF-β1 in either a Smad4-dependent or -independent manner. Molecules that were modulated >2 or <0.5-fold by the stimuli were considered to be targets of TGF-β1. Of the 3756 arrayed genes, 187 from the S4KD cells and 155 from the WT cells were identified as targets of TGF-β1. In all, 22 genes were obtained from the two cell types, including nine commonly upregulated, four commonly downregulated, and nine inversely regulated genes

Smad4-dependent and -independent target genes of TGF-β (Figure 6, Table 2). In all, 22 clones were obtained from the S4KD and WT cells. Of these, nine clones were commonly upregulated and four clones were commonly downregulated; these clones were considered to be regulated in a Smad4-independent manner. The remaining nine clones were found to be inversely regulated between the S4KD and WT cells (Figure 6).

Based on a survey of published reports on the relationships between various molecules and TGF-β, including the previous microarray data on TGF-β signaling (Akiyoshi *et al*., 2001; Chen *et al*., 2001; Verrecchia *et al*., 2001; Zavadil *et al*., 2001), we conclude that 246 of the identified genes have not been reported previously as genes that lie downstream of TGF-β1. In particular, we found 142 novel targets among the 187 Smad4-independent target molecules that were regulated by TGF-β1, which have not been previously reported, even in Smad4 intact cells.

We also performed proteomic analysis of the S4KD cells (Imamura *et al*., 2004). The 12 previously identified target molecules of TGF-β1 showed no overlap with those identified in this study due to the fact that the arrayed genes screened were a small fraction of the whole genome, and also because, in part, the protein samples in the previous study were harvested after a 12-h incubation with TGF-β1; our RNA samples, however, were collected after 2 h of TGF-β1 stimulation. Moreover, discrepancies between mRNA and protein levels have been found in previous studies, which is indicative of the translational and post-translational regulation of each molecule (Gygi *et al*., 1999; Chen *et al*., 2002).

Although the existence of a non-Smad pathway downstream of TGF-β has been demonstrated (Hartsough and Mulder, 1995; Engel *et al*., 1999; Hocevar *et al*., 1999; Bhowmick *et al*., 2001; Yu *et al*., 2002), it has not been elucidated to the same extent as the Smad pathway. In the present study, the microarray data showed that TGF-β1 immediately up- or downregulated 4–5% of the 3756 arrayed genes in the Smad4 intact and Smad4-inactivated cells. This result suggests that the Smad4-dependent and -independent pathways are of

comparative importance, based on the number of regulated genes.

Given our results, how is the TGF-β signal transmitted independently of Smad4? We propose two possible pathways. First, the signal may pass via the TβRI-Smad2/3 pathway. We have recently shown that p21/WAF1 may be upregulated by TGF-β in a Smad4-independent manner through TβRI-Smad2/3 signaling and not via the mitogen-activated protein kinase cascade (Ijichi *et al.*, 2004). A novel, alternative Co-Smad may be involved in this pathway. Second, a non-Smad pathway that transmits the signal in a Smad2/3/4-independent manner. In terms of non-Smad pathways, p38, c-Jun amino-terminal kinase, and Rho have been implicated in TGF-β-induced apoptosis, epithelial–mesenchymal transition, cell motility, and cancer cell invasion (Bhowmick *et al.*, 2001; Yu *et al.*, 2002).

Gene function profiles induced by TGF-β1 signaling in the S4KD and Smad4 intact cells

All of the target genes that were identified in the microarray were classified according to biological function (Table 3). Molecules that are involved in signal transduction, transcription, and metabolism were frequently observed in both the S4KD and WT arrays. As shown in Table 3, molecules that are associated with positive or negative cell proliferation showed different patterns of expression between the S4KD and WT cells. Unexpectedly, molecules related to positive cell proliferation were upregulated frequently in Smad4 intact cells, whereas these molecules were downregulated frequently in S4KD cells. This suggests that TGF-β may regulate target molecules that are involved in proapoptosis and growth inhibition, as well as those associated with antiapoptosis and growth stimulation, and thereby exert extensive control over complicated biological functions. The results are complex, because some of the genes that we classified as being involved in either positive or negative cell proliferation have been reported as being both proapoptotic and antiapoptotic, depending on the cell state; in addition, some of these genes have been reported exclusively in certain none-pithelial cell types.

Table 3 Classification of TGF-β1-targeted genes in PANC-1-S4KD and PANC-1-puro cells

Gene function	*PANC-1-S4KD*		*PANC-1-puro*	
	Up	*Down*	*Up*	*Down*
Cell adhesion	2	3	3	0
Cell motility	5	0	0	0
Cell structure	3	2	2	1
Cell death or antiproliferation	6	3	4	1
Positive cell proliferation	4	5	8	1
Signal transduction	21	22	24	5
Transcription	21	2	14	4
Metabolism	16	5	17	9
Molecule transport	10	7	14	4
Others	11	7	8	7
Unknown	21	11	22	7
Total	120	67	116	39

Table 3 shows that cell adhesion molecules were downregulated frequently, and that molecules that promote cell motility were upregulated frequently in S4KD cells in response to TGF-β1, which suggests that these cells may separate from the primary tumor and invade the surrounding tissues.

Moreover, inverse regulation patterns between the S4KD and WT cells were seen for nine genes, which included genes that are associated with cell adhesion, positive cell proliferation, and signal transduction. These target genes may be up- or downregulated by TGF-β1 via the Smad4 intact pathway, and may be inversely regulated due to Smad4 inactivation. The modulation of these target genes may produce the malignant characteristics of pancreatic cancer cells, although this remains to be investigated.

Cell migration induced by TGF-β1 was inhibited in the S4KD cells

In order to elucidate the phenotypic change that was due to the S4KD, we performed the following *in vitro* and *in vivo* assays. First, cell proliferation was examined using the MTT (methylthiazolyl diphenyl-tetrazolium bromide) and BrdU (5-bromo-2′-deoxyuridine) incorporation assays. A transwell cell invasion assay using a Matrigel-coated chamber (BD Biosciences, San Jose, CA, USA) was also performed. However, the results of these assays showed no significant differences between the S4KD and WT cells (data not shown). Then, we performed a more precise cell cycle analysis after synchronizing the cell phase using a modified thymidine block method. In brief, cells were incubated with 2.5 mM thymidine for 24 h, then after 14 h, they were incubated with 10 μg/ml aphidicolin for another 14 h, which synchronized most of the cells in the G1 phase. Then the cells were treated with or without 5 ng/ml TGF-β1 and S phase entry was analysed using flow cytometry. TGF-β1 clearly inhibited S phase entry not only in WT cells but also in S4KD cells, and the difference was not significant (data not shown).

Our attempts to implant these cells subcutaneously in nude mice and severely compromised immunodeficient (SCID) mice were unsuccessful. Then, we injected the cells into the spleens of nude and SCID mice to examine whether they could metastasize to the liver. On killing the mice after 6 weeks, no metastasis was found.

Finally, we performed an *in vitro* cell migration assay (wound closure assay) as described in Materials and methods. TGF-β is associated with cell migration in certain cell lines (Morton and Barrack, 1995; Dumont *et al.*, 2003). In this study, the WT cells also migrated rapidly with the stimuli, while the S4KD cells showed obviously delayed migration (Figure 7). The count of the cells showed no difference in number between these cells. We performed the experiment five times, and the results were similar. Since PANC-1 (parental cells) also showed rapid migration, the delay due to S4KD was considered a phenotypic change due to the S4KD. In

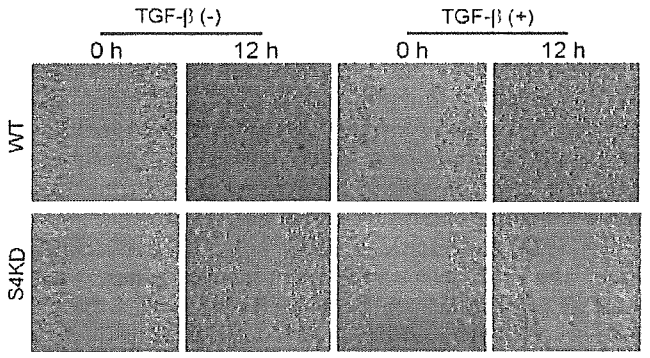

Figure 7 Cell migration assay on the S4KD and Smad4 intact cell lines. The cells were seeded and incubated with or without 5 ng/ml TGF-β1 for 24 h. Then, confluent cell monolayers were wounded by scraping, using a pipette tip with the same width, and the cell migration was observed at various times. Each experiment was repeated five times and the representative result is shown. Magnification: $\times 40$

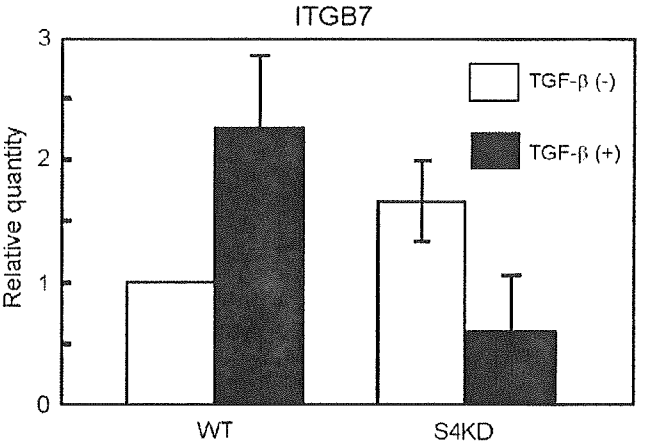

Figure 8 Quantitative RT–PCR of integrin β7. Quantitative RT–PCR analysis of integrin β7 (ITGB7) was performed as described above. The ratio of the mRNA level of ITGB7 to that of GAPDH was calculated, and the value of 1.0 was assigned to WT cells that were incubated without TGF-β1. The experiments were repeated twice in triplicate, and the mean and s.d. are shown. Bar, s.d.

some cell lines, the TGF-β-induced migration was Smad-independent (Dumont *et al.*, 2003); by contrast, the PANC-1 cell family demonstrated Smad4-dependent migration.

Following this, we performed quantitative RT–PCR analysis of the genes that were inversely regulated in the microarray, and found that integrin β7 (ITGB7), which is one of the integrin family, was upregulated by TGF-β1 in WT cells, but downregulated in S4KD cells (Figure 8). The integrin family members are cell adhesion molecules, and have a dual effect promoting and preventing cell migration (Jin and Varner, 2004). Certain subclasses of the family are upregulated by TGF-β (Xie *et al.*, 2003) and so is ITGB7 in T cells (Lim *et al.*, 1998), although the exact function of ITGB7 in epithelial cells is not completely understood. Our study suggested that the regulation of ITGB7 plays a role in cell migration, although it remains unclear whether the inhibition of cell migration due to the loss of Smad4 function is be associated with the malignant character of pancreatic cancer.

As described above, we detected a number of distinct target genes in our study that were regulated downstream of the TGF-β signal. The significance and mechanism of TGF-β-induced regulation of each target gene should be investigated further in order to achieve a better understanding of pancreatic cancer. A comprehensive understanding of the intracellular dynamics of pancreatic cancer should lead to the development of novel therapeutic targets with clinical relevance.

Materials and methods

Cell culture

The pancreatic cancer cell line PANC-1 was purchased from the American Type Culture Collection (Rockville, MD, USA). It was maintained in Dulbecco's modified Eagle's medium (Sigma, St Louis, MO, USA) supplemented with 10% fetal bovine serum (Sigma) at 37°C in a 5% CO_2 atmosphere.

Plasmids

The pcPUR + U6icassette, pCMV5-Smad4-Flag, and $(CAGA)_9$-luc plasmids were described previously (Dennler *et al.*, 1998; Ijichi *et al.*, 2001; Miyagishi and Taira, 2002; Yokota *et al.*, 2003). The pRL-SV40 vector (Promega, Madison, WI, USA), which contains the SV40 promoter upstream of the coding sequence of *Renilla* luciferase, was used as the internal control in the luciferase assay.

Transfection

Transfection into the cells was performed in this study using the transfection reagent Effectene (Qiagen, Hilden, Germany) according to the manufacturer's instructions.

Western blotting

Western blotting was performed as described previously (Ijichi *et al.*, 2001). The equal amounts of protein were electrophoresed and the Smad4 and β-actin proteins were detected with the anti-Smad4 antibody (BD Transduction Laboratories, Lexington, KY, USA) at a dilution of 1 : 250 or anti-β-actin antibody (Sigma) at a dilution of 1 : 2500.

Luciferase assay

The PANC-1-S4KD and WT cells were transfected with $(CAGA)_9$-luc and pRL-SV40. After 24 h, the cells were incubated with or without 2.5 ng/ml TGF-β1 (R&D Systems, Minneapolis, MN, USA) for an additional 24 h, and the dual luciferase assay was performed as described previously (Ijichi *et al.*, 2001). The firefly luciferase activity of $(CAGA)_9$-luc was normalized to the *Renilla* luciferase activity of pRL-SV40. The level of luciferase in cells in the absence of TGF-β1 was assigned a value of 1.0, and the relative activities were calculated. The experiments were performed twice in duplicate.

Quantitative RT–PCR

The PANC-1-S4KD and WT cell pools were incubated with or without 10 ng/ml of TGF-β1 for 2 h, and the total RNA was

extracted from these cells using ISOGEN (Nippon Gene, Tokyo, Japan). The cDNA templates were synthesized from 1 μg of total RNA using the ImProm-II™ Reverse Transcription System (Promega). Quantitative RT–PCR analysis was performed using the ABI 7000 Real-Time PCR System (Applied Biosystems, Foster City, CA, USA), according to the manufacturer's instructions. The ratio of the mRNA level of each gene to that of glyceraldehyde-3-phosphate dehydrogenase (GAPDH) was calculated, and the value of 1.0 was assigned to the WT cells that were incubated without TGF-β1. Each experiment was repeated twice in triplicate. The primer sequences are shown in Supplementary Table 2.

cDNA microarray

The PANC-1-S4KD and WT cell pools were incubated for 2 h in the presence or absence of 10 ng/ml TGF-β1, and total RNA was extracted. The following samples were obtained: (i) S4KD cells incubated without TGF-β1; (ii) S4KD cells stimulated with TGF-β1; (iii) WT cells incubated without TGF-β1; and (iv) WT cells stimulated with TGF-β1. The microarray procedure was performed using the Atlas Glass Array Human 3.8 II Microarray (Clontech, Palo Alto, CA, USA), according to the manufacturer's instructions. In brief, cDNA probes were prepared from 7 μg of the total RNA, and labeled with the fluorescent dye Cy3 (Amersham Biosciences, Uppsala, Sweden) using the PowerScript Reverse Transcription Kit (Clontech). The samples were then applied onto the microarray followed by incubation at 50°C overnight under humid conditions. After washing, fluorescence images of the microarrays were scanned with a fluorescence laser confocal slide scanner (Affymetrix 428 Array Scanner; Affymetrix, Santa Clara, CA, USA). The Cy3 intensities with background subtraction were determined in each sample and the results were compared each other using ImaGene 4.2 software (BioDiscovery, Marina Del Rey, CA, USA). The comparison analysis was performed after normalization by the total Cy3 intensities. We repeated hybridizations four times per each sample and used the most reliable pair of hybridizations that showed high and almost equal total intensities in order to avoid a critical bias for the data. The analyses with probes (ii) and (i) were compared to detect clones that were putatively regulated in a Smad4-independent manner by TGF-β1. Comparison of the analyses with probes (iv) and (iii) identified clones that were putatively regulated by TGF-β1 in either a Smad4-dependent or -independent manner. Molecules that were modulated >2- or <0.5-fold by the stimuli were considered to be targets of TGF-β1.

Cell migration assay (wound closure assay)

A total of 10^6 cells were seeded and incubated with or without 5 ng/ml TGF-β1 for 24 h. Then confluent cell monolayers were wounded by scraping, using a pipette tip with the same width, and the cell migration was carefully observed at various times. Each experiment was repeated five times.

Acknowledgements
We thank R Derynck for providing the plasmid and M Tsubouchi for technical assistance. This study was supported by the Japanese Ministry of Education, Culture, Sports, Science, and Technology (MEXT).

References

Akiyoshi S, Ishii M, Nemoto N, Kawabata M, Aburatani H and Miyazono K. (2001). *Jpn. J. Cancer Res.*, **92,** 257–268.
Bhowmick NA, Ghiassi M, Bakin A, Aakre M, Lundquist CA, Engel ME, Arteaga CL and Moses HL. (2001). *Mol. Cell Biol.*, **12,** 27–36.
Brummelkamp TR, Bernards R and Agami R. (2002). *Science*, **296,** 550–553.
Chen G, Gharib TG, Huang C-C, Taylor JMG, Misek DE, Kardia SLR, Giordano TJ, Iannettoni MD, Orringer MB, Hanash SM and Beer DG. (2002). *Mol. Cell. Proteomics*, **1,** 304–313.
Chen CR, Kang Y and Massague J. (2001). *Proc. Natl. Acad. Sci. USA*, **98,** 992–999.
Dennler S, Itoh S, Vivien D, ten Dijke P, Huet S and Gauthier JM. (1998). *EMBO J.*, **17,** 3091–3100.
Derynck R, Akhurst RJ and Balmain A. (2001). *Nat. Genet.*, **29,** 117–129.
Derynck R, Goeddel DV, Ullrich A, Gutterman JU, Williams RD, Bringman TS and Berger WH. (1983). *Cancer Res.*, **47,** 707–712.
Dumont N, Bakin A and Arteaga CL. (2003). *J. Biol. Chem.*, **278,** 3275–3285.
Elbashir SM, Harborth J, Lendeckel W, Yalcin A, Weber K and Tuschl T. (2001). *Nature*, **411,** 494–498.
Engel ME, McDonnell MA, Law BK and Moses HL. (1999). *J. Biol. Chem.*, **274,** 37413–37420.
Friess H, Yamanaka Y, Buchler M, Ebert M, Beger HG, Gold LI and Korc M. (1993). *Gastroenterology*, **105,** 1846–1856.
Grau AM, Zhang L, Wang W, Ruan S, Evans DB, Abbruzzese JL, Zhang W and Chiao PJ. (1997). *Cancer Res.*, **57,** 3929–3934.
Gygi SP, Rochon Y, Franza BR and Aebersold R. (1999). *Mol. Cell. Biol.*, **19,** 1720–1730.
Hahn SA, Schutte M, Hoque ATMS, Moskaluk CA, da Costa LT, Rozenblum E, Weinstein CL, Fischer A, Yeo CJ, Hruban RH and Kern SE. (1996). *Science*, **271,** 350–353.
Hartsough MT and Mulder KM. (1995). *J. Biol. Chem.*, **270,** 7117–7124.
Hocevar BA, Brown TL and Howe PH. (1999). *EMBO J.*, **18,** 1345–1356.
Ijichi H, Ikenoue T, Kato N, Mitsuno M, Togo G, Kato J, Kanai F, Shiratori Y and Omata M. (2001). *Biochem. Biophys. Res. Commun.*, **289,** 350–357.
Ijichi H, Otsuka M, Kanai F, Ikenoue T, Tateishi K, Kawakami T, Arakawa Y, Shimizu K, Miyazono K, Kawabe T and Omata M. (2004). *Oncogene*, **23,** 1043–1051.
Imamura T, Kanai F, Kawakami T, Amarsanaa J, Ijichi H, Hoshida Y, Tanaka Y, Ikenoue T, Tateishi K, Kawabe T, Arakawa Y, Miyagishi M, Taira K, Yokosuka O and Omata M. (2004). *Biochem. Biophys. Res. Commun.*, **318,** 289–296.
Jackson AL, Bartz SR, Schelter J, Kobayashi SV, Burchard J, Mao M, Li B, Cavet G and Linsley PS. (2003). *Nat. Biotechnol.*, **21,** 635–637.
Jin H and Varner J. (2004). *Br. J. Cancer*, **90,** 561–565.
Lim SP, Leung E and Krissansen GW. (1998). *Immunogenetics*, **48,** 184–195.
Markowitz S, Wang J, Myeroff L, Parsons R, Sun L, Lutterbaugh J, Fan RS, Zborowska E, Kinzler W, Vogelstein B, Brattain M and Willson JKV. (1995). *Science*, **268,** 1336–1338.
Miyagishi M and Taira K. (2002). *Nat. Biotech.*, **19,** 497–500.

Miyaki M, Iijima T, Konishi M, Sakai K, Ishii A, Yasuno M, Hishima T, Koike M, Shitara N, Iwama T, Utsunomiya J, Kuroki T and Mori T. (1999). *Oncogene*, **18,** 3098–3103.

Miyazono K, ten Dijke P and Heldin CH. (2000). *Adv. Immunol.*, **75,** 115–157.

Morton DM and Barrack ER. (1995). *Cancer Res.*, **55,** 2596–2602.

Schutte M, Hruban RH, Hedrick L, Cho KR, Nadasdy GM, Weinstein CL, Bova GS, Isaacs WB, Cairns P, Nawroz H, Sidransky D, Casero Jr RA, Meltzer PS, Hahn SA and Kern SE. (1996). *Cancer Res.*, **56,** 2527–2530.

Togo G, Toda N, Kanai F, Kato N, Shiratori Y, Kishi K, Imazeki F, Makuuchi M and Omata M. (1996). *Cancer Res.*, **56,** 5620–5623.

Verrecchia F, Chu ML and Mauviel A. (2001). *J. Biol. Chem.*, **276,** 17058–17062.

Wang D, Kanuma T, Mizunuma H, Takama F, Ibuki Y, Wake N, Mogi A, Shitara Y and Takenoshita S. (2000). *Cancer Res.*, **60,** 4507–4512.

Xie L, Law BK, Aakre ME, Edgerton M, Shyr Y, Bhowmick NA and Moses HL. (2003). *Breast Cancer Res.*, **5,** R187–R198.

Yokota T, Sakamoto N, Enomoto N, Tanabe Y, Miyagishi M, Maekawa S, Yi L, Kurosaki M, Taira K, Watanabe M and Mizusawa H. (2003). *EMBO Rep.*, **4,** 602–608.

Yu L, Hebert C and Zhang YE. (2002). *EMBO J.*, **21,** 3749–3759.

Zavadil J, Bitzer M, Liang D, Yang YC, Massimi A, Kneitz S, Piek E and Boettinger EP. (2001). *Proc. Natl. Acad. Sci. USA*, **98,** 6686–6691.

Supplementary Information accompanies the paper on Oncogene website (http://www.nature.com/onc)

Blockade of the Stromal Cell–Derived Factor-1/CXCR4 Axis Attenuates *In vivo* Tumor Growth by Inhibiting Angiogenesis in a Vascular Endothelial Growth Factor–Independent Manner

Bayasi Guleng,[1] Keisuke Tateishi,[1] Miki Ohta,[1] Fumihiko Kanai,[1,5] Amarsanaa Jazag,[1] Hideaki Ijichi,[1] Yasuo Tanaka,[1] Miwa Washida,[2] Keita Morikane,[6] Yasushi Fukushima,[1] Takao Yamori,[7] Takashi Tsuruo,[3] Takao Kawabe,[1] Makoto Miyagishi,[4,8] Kazunari Taira,[4,8] Masataka Sata,[2] and Masao Omata[1]

[1]Department of Gastroenterology and [2]Cardiovascular Medicine, Graduate School of Medicine, [3]Institute of Molecular and Cellular Biosciences, and [4]Department of Chemistry and Biotechnology, Graduate School of Engineering, University of Tokyo; [5]Clinical Research Center, University of Tokyo Hospital; [6]Infectious Disease Surveillance Center, National Institute of Infectious Diseases; and [7]Division of Molecular Pharmacology, Cancer Chemotherapy Center, Japanese Foundation for Cancer Research, Tokyo, Japan and [8]Gene Discovery Research Center, National Institute of Advanced Industrial Science and Technology, Tsukuba, Japan

Abstract

The interaction between the chemokine receptor CXCR4 and its specific ligand, stromal cell–derived factor-1 (SDF-1/CXCL12), mediates several cellular functions. In cancer, SDF-1-positive or CXCR4-positive cells of various lineages are detected within tumor tissues. Recent intensive research has indicated the possibility that blocking CXCR4 could reduce the metastatic potential of cancer cells. Here, we show that the inhibition of the SDF-1/CXCR4 axis decreases the growth of s.c. gastrointestinal tumors through the suppression of tumor neoangiogenesis. The neutralization of CXCR4 suppressed the growth *in vivo* of tumors derived from mouse Colon38 and PancO2 cells, whereas it did not affect the growth of Colon38 and PancO2 cells *in vitro*. This attenuation of tumor growth was found to be independent of the expression of CXCR4 by the cancer cells themselves, because CXCR4 knocked-down Colon38 cells grew similarly to control cells. Furthermore, CD31-positive tumor capillaries were reduced to 45% ($P < 0.001$) and intratumor blood flows were decreased to 65% ($P < 0.01$) by blockade of CXCR4. The vascular endothelial growth factor (VEGF) concentration in the tumors was not affected by the neutralization of CXCR4. Taken together with the detection of CXCR4-positive endothelial cells in the tumor tissues, the findings suggest that the antiangiogenic effects of the blockade of CXCR4 are related to a reduction of the establishment of tumor endothelium independently of VEGF inhibition. Our data indicate that the SDF-1/CXCR4 pathway might be a general target for anticancer strategies and that blocking this system could be cooperatively effective in combination with other antiangiogenic therapies, such as blockade of VEGF. (Cancer Res 2005; 65(13): 5864-71)

Introduction

The chemokines are a group of chemoattractant cytokines that mediate several cellular functions. Stromal cell–derived factor-1α (SDF-1) is expressed by stromal cells, including fibroblasts and endothelial cells (1, 2), and interacts specifically with the seven-transmembrane, G protein–coupled receptor CXCR4 (3). CXCR4 is expressed in various cells, such as T lymphocytes, monocytes, neutrophils (4), and endothelial cells (5, 6). On ligand binding, CXCR4 activates several signaling cascades, including the phosphatidylinostiol 3-kinase and mitogen-activated protein kinase cascades, which induce cytoskeletal rearrangement, antiapoptosis effects, and cell growth (7). Importantly, the SDF-1/CXCR4 interaction is critical for the homing and retention of hematopoietic stem cells within the bone marrow and is essential in fetal hematopoiesis (8).

Recently, intensive research has indicated that CXCR4 is involved in increasing the metastatic potential of colon and breast cancer cells (2, 9, 10). For example, *CXCR4* was one of the few genes that was up-regulated in bone-metastasized breast cancer cells (11), and cells that had metastasized to the lungs expressed very high levels of CXCR4 compared with the parental tumor cells. Another study found that SDF-1 was up-regulated in malignant tissues (12). *In vivo*, neutralizing the interaction of CXCR4 and SDF-1 significantly impaired the metastasis of breast cancer cells and cell migration (2). These findings suggest the possibility that inhibition of the SDF-1/CXCR4 axis could be a strategy for the prevention of cancer cell metastasis. The mechanism by which CXCR4 expression enhances tumor metastasis is still unclear; however, the activation of CXCR4 by SDF-1 seems to have the ability to trigger the adhesion of a variety of tumor cell lines to extracellular matrix substrates, such as fibronectin (13, 14), and to vascular endothelial cells by increasing the vascular permeability (12, 15).

Tumor neovascularization, a rate-limiting step in cancer progression, is thought to be established by the sprouting of blood vessels through the division of differentiated endothelial cells. However, the growth of new vessels can be mediated in several ways. Recently, circulating endothelial progenitor cells mobilized from the bone marrow were detected in the peripheral blood of several species and were implicated in the neoangiogenesis involved in tumorigenesis as well as in the formation of new vessels after trauma, burn injury, and myocardial infarction (16–18). The SDF-1/CXCR4 axis mediates the guidance of primordial stem cells to sites of rapid vascular expansion during embryonic organogenesis (19). An analysis of CXCR4-deficient mice revealed that the receptor was essential for fetal gastrointestinal vascular formation (20), suggesting a pivotal role of the SDF-1/CXCR4 axis in fetal angiogenesis (8). Like embryonic vasculogenesis, tumor angiogenesis might be mediated by various progenitor cells

Requests for reprints: Keisuke Tateishi, Department of Gastroenterology, Graduate School of Medicine, University of Tokyo, 7-3-1 Hongo, Bunkyo-ku, Tokyo 113-8655, Japan. Phone: 81-3-3815-5411, ext. 30237; Fax: 81-3-3814-0021; E-mail: tateishik-int@h.u-tokyo.ac.jp.

(21). We analyzed the contribution of the SDF-1/CXCR4 interaction to tumor neoangiogenesis using a mouse model. Here, we show that the *in vivo* neutralization of CXCR4 also results in the attenuation of tumor growth by the inhibition of tumor neovascularization in a vascular endothelial growth factor (VEGF)–independent manner regardless of whether the cancer cells express CXCR4. CXCR4-targeting therapy might be applied as an antiangiogenic strategy for treatment of a broad spectrum of cancers.

Materials and Methods

Animals and cells. All C57BL/6 mice and BALB/c nude mice were purchased from Clea Corp. (Tokyo, Japan). The transgenic mice (C57BL/6 background) that ubiquitously expressed enhanced green fluorescent protein (GFP mice) were a generous gift from Dr. Masaru Okabe (Osaka University, Osaka, Japan; ref. 22). All procedures involving experimental animals were done in accordance with protocols approved by the Institutional Committee for Animal Research of the University of Tokyo and complied with the USPHS *Policy on Humane Care and Use of Laboratory Animals*. Colon38 (23) and PancO2 (24) cells are colon and pancreatic cancer cells, respectively, derived from C57BL/6 mice. PancO2 cells were obtained from Dr. Michael A. Hollingsworth (Eppley Institute, University of Nebraska, Omaha, NE).

Stable knockdown of CXCR4. A plasmid carrying RNA interference targeted to mouse CXCR4 was constructed as described previously (25, 26). The siCXCR4 sequence of the mouse *CXCR4* gene (5′-GCAAAGACTTATA-TAATATAT-3′) was selected using our original algorithm. Colon38 cells were transfected with pcPUR+U6-siCXCR4 or pcPUR+U6-siRenilla (control) and selected as puromycin-resistant pools. Then, quantitative reverse transcription-PCR (RT-PCR) was done to confirm the CXCR4 mRNA suppression using the primers 5′-TCAGCCTGGACCGGTACCT-3′ and 5′-GCAGTTTCC-TTGGCCTTTGA-3′.

Bone marrow transplantation and tumor implantation model. The bone marrow of lethally irradiated C57BL/6 mice was reconstituted by transplantation with bone marrow cells from GFP mice (GFP-BMT mice). Briefly, wild-type C57BL/6 mice were lethally irradiated with a total dose of 950 rads (MBR-1520RB, Hitachi, Tokyo, Japan; ref. 27); then, 2×10^6 bone marrow cells from GFP mice were injected into the tail veins of the irradiated recipient mice. The bone marrow cells of the GFP-BMT mice were sampled at 4 weeks after bone marrow transplantation, and the degree of chimerism was investigated by flow cytometry (EPICS XL, Beckman Coulter, Fullerton, CA). More than 85% of the cells in the recipient bone marrow were GFP positive using these experimental conditions (data not shown). Tumors were induced by s.c. injection of 2×10^6 cancer cells into the flank >4 weeks after the bone marrow transplantation. Large tumors were typically observed by 4 weeks after tumor implantation. The mice were anesthetized with pentobarbital sodium (120 mg/kg), and the tumor tissues were harvested for histologic analysis.

Isolation of tumor-infiltrating cells and reverse transcription-PCR analysis. Tumor-infiltrating cells (TIC) were isolated from the tumors formed by Colon38 and PancO2 cells using density gradient centrifugation in Percoll/RediGrad (Amersham Biosciences, Buckinghamshire, United Kingdom) as described previously (28). The total RNA was extracted from the TICs using ISOGEN reagent (Nippon Gene Co., Tokyo, Japan), and the reverse transcription reaction and PCR amplification were done as described (29). The PCR primer sequences were as follows: sense 5′-GGCTGTAGAGCGAGTGTTGC-3′ and antisense 5′-GTAGAGGTTGA-CAGTGTAGAT-3′ for CXCR4 (29) and sense 5′-GTTGGATACAGGCCA-GACTTTGTTG-3′ and antisense 5′-GATTCAACTTGCGCTCATCTTAGGC-3′ for hypoxanthine phosphoribosyltransferase (HPRT).

Immunohistochemistry. Tumor tissue samples were fixed in 2% paraformaldehyde and embedded with a Technovit catalyst system (Heraeus Kulzer GmbH & Co. KG, Wehrheim, Germany; ref. 30). The primary antibodies were as follows: rabbit anti-rat CXCR4 (Torrey Pines Biolabs, Inc., Houston, TX), rabbit anti-mouse CXCR4 (H-118) and anti-VEGF (sc-507; Santa Cruz Biotechnology, Santa Cruz, CA), rabbit anti-mouse SDF-1α (Torrey Pines Biolabs), rat anti-mouse CD31 (BD PharMingen, San Diego, CA), and rat anti-mouse Mac3 (BD PharMingen). The secondary antibodies were conjugated with fluorochrome Alexa Fluor 488 or 555 (Molecular Probes, Inc., Eugene, OR). The sections were observed under a confocal microscope (Leica Microsystems, Wetzlar, Germany; ref. 31).

***In vivo* neutralizing antibody studies.** Cancer cells (Colon38 or PancO2; 8×10^6) were s.c. injected into BALB/c nude mice. One group of tumor-bearing mice ($n = 5$) then received an i.p. injection of 10 μg rabbit anti-rat CXCR4-neutralizing antibody, which is reported to also bind to murine CXCR4 (32). The control group of tumor-bearing mice received 10 μg normal rabbit IgG. The mice were treated every 24 hours starting on day 3 for a total of eight separate injections of anti-CXCR4 antibody. The tumor size was measured, and the volume was calculated as [length (mm) × width $(mm)^2$] / 2. The experiments were also done using C57BL/6 mice ($n = 4$).

3-(4,5-Dimethylthiazol-2-yl)-2,5-diphenyltetrazolium bromide assay. The direct effect of the neutralizing antibody on the viability of the tumor cells was assessed by seeding 3×10^4 Colon38 cells in 24-well microplates and replacing the medium with medium containing 10 μg/mL normal IgG or 10 μg/mL anti-CXCR4-neutralizing antibody ($n = 3$) after 24 hours. The number of viable cells was determined using the 3-(4,5-dimethylthiazol-2-yl)-2,5-diphenyltetrazolium bromide (MTT) assay (Sigma, St. Louis, MO) at 24, 48, and 72 hours (33). Similarly, a total of 3×10^4 Colon38-siCXCR4 or Colon38-siRenilla cells were cultured with 300 ng/mL recombinant human SDF-1α (PeproTech EC, London, United Kingdom) in 24-well microplates, and the number of viable cells was analyzed using the MTT assay at 24, 48, and 72 hours.

Fluorescent phalloidin staining. A total of 10^5 Colon38 or PancO2 cells were seeded in two-well chambers and incubated with 10 μg/mL normal IgG or 10 μg/mL anti-CXCR4-neutralizing antibody with 300 ng/mL recombinant human SDF-1α for 24 hours; then, the cells were stained with Alexa Fluor 488–labeled phalloidin according to the manufacturer's instructions.

Cell migration assay (wound closure assay). A total of 10^5 Colon38 or PancO2 cells were seeded in two-well chambers, and confluent cell monolayers were wounded by scraping using a pipette tip of the same width and replacing the medium with medium containing 10 μg/mL normal IgG or 10 μg/mL anti-CXCR4-neutralizing antibody with 300 ng/mL recombinant human SDF-1α for 24 hours. Then, the cells were fixed and stained with Diff-Quick, and cell migration was observed using bright-field microscopy at ×40 magnification.

Quantitative reverse transcription-PCR. A total of 5×10^5 Colon38 or PancO2 cells were seeded in 6-cm dishes and incubated with 10 μg/mL normal IgG or 10 μg/mL anti-CXCR4-neutralizing antibody for 24 hours. The total RNA was extracted, treated with DNase, and purified. Quantitative RT-PCR analysis was done using an ABI 7000 Real-time PCR System (Applied Biosystems, Foster City, CA). The mRNA level of each gene was normalized to HPRT. The primers were as follows: basic fibroblast growth factor (bFGF), forward 5′-CACCAGGCCACTTCAAGGA-3′ and reverse 5′-GATGGATGCGCAGGAAGAA-3′; platelet-derived growth factor (PDGF), forward 5′-AAGCTCGGGTGACCATTCG-3′ and reverse 5′-ACTTT-CGGTGCTTGCCTTTG-3′; and placenta growth factor (PlGF), forward 5′-CCCTGTCTGCTGGGAACAA-3′ and reverse 5′-GCTGCGACCCCA-CACTTC-3′. The SDF-1, matrix metalloproteinase-9 (MMP-9), intercellular adhesion molecule (ICAM), and VCAM (VCAM) primer sequences were reported previously (34).

Late-outgrowth endothelial colony assay. To isolate the peripheral blood mononuclear cells (PBMC; ref. 18), blood samples (500-1,000 μL) from mice were collected in heparinized tubes ~3 weeks after tumor implantation. The PBMCs were isolated by Ficoll gradient centrifugation (Amersham Biosciences AB, Uppsala, Sweden). To detect circulating endothelial cells, 3×10^5 freshly isolated PBMCs were cultured in modified endothelial growth medium (EGM), which was composed of X-vivo-20 serum-free medium with VEGF (10 ng/mL, R&D, Minneapolis, MN), endothelial cell growth supplement (30 μg/mL, Upstate, Lake Placid, NY), human recombinant bFGF (5 ng/mL, Invitrogen, Carlsbad, CA), heparin